FUNCTIONALIZED ELECTROSPUN NANOFIBERS IN MICROFLUIDIC BIOANALYTICAL SYSTEMS

A Thesis

Presented to the Faculty of the Graduate School

of Cornell University

in Partial Fulfillment of the Requirements for the Degree of

Master of Science

By

Lauren Elizabeth Matlock-Colangelo

January 2012

ABSTRACT

Biosensors detect target analytes through specific binding with biological recognition elements such as nucleic acids, enzymes, and antibodies. Many labs are working to create inexpensive and portable miniaturized sensors that allow for rapid sample analysis and low reagent consumption in order to increase biosensor accessibility in rural areas and third world countries. Lab-on-a-chip devices aim to incorporate sample preparation and analyte detection into one device in order to create self-contained sensors that can be used in rural areas and third world countries where laboratory equipment may not be available. Often, these devices incorporate microfluidics in order to shorten reaction times, reduce handling of hazardous samples, and take advantage of laminar flow [1]. However, while several successful lab-on-a-chip devices have been developed, incorporating sample preparation and analyte detection within one device is still a key challenge in the design of many biosensors. Sample preparation is extremely important for miniaturized sensors, which have a low tolerance for sample impurities and particulates [1]. In addition, significant sample concentration is often required to reduce sample volumes to the nL to mL range used in miniaturized sensors. This research aims to address the need for sample preparation within lab-on-a-chip systems through the use of functionalized electrospun nanofibers within polymer microfluidic devices.

Electrospinning is a fiber formation process that uses electrical forces to form fibers with diameters on the order of 100 nm from polymer spinning dopes [2, 3]. The non-woven fiber mats formed during electrospinning have extremely high surface area to volume ratios, and can be used to increase the sensitivity and binding capacity of biosensors without increasing their size. Additionally, the fibers can be functionalized through the incorporation of nano and microscale materials within a polymer spinning dope. In this work, positively and negatively charged

nanofibers were created through the incorporation of hexadimethrine bromide (polybrene) and poly(maleic anhydride) (Poly(MA)) within a poly(vinyl alcohol) spinning dope. Fourier transform infrared spectroscopy (FTIR) and X-ray photoelectron spectroscopy (XPS) confirmed the successful incorporation of polybrene and poly(MA) into the nanofibers.

Gold microelectrodes were patterned on poly(methyl methacrylate) (PMMA) to facilitate the incorporation of nanofibers within microfluidic devices. The gold microelectrodes served as grounded collector plates during electrospinning and produced well-aligned nanofiber mats. Microchannels 1 mm wide and 52 μm deep were imprinted into PMMA through hot embossing with a copper template. PMMA pieces embossed with microchannels were bonded to PMMA pieces with gold microelectrodes and nanofibers using UV-assisted thermal bonding.

Positively charged polybrene-modified nanofibers were shown to successfully filter negatively charged fluorescent liposomes out of a HEPES-sucrose-saline buffer, while negatively charged poly(MA)-modified nanofibers were shown to repel the liposomes. The effect of nanofiber mat thickness on liposome retention was studied using the z-scan function of a Leica confocal microscope. It was determined that positively charged nanofibers exhibited optimal liposome retention at thicknesses of 20 μm and above. Negatively charged nanofiber mats over 40 μm thick retained liposomes due to their small pore size despite their surface charge. Finally, it was demonstrated that a HEPES-sucrose-saline solution of pH 8.5 could be used to change the charge of the positively charged polybrene nanofibers and allow for the release of previously bound liposomes.

The results of this study can be used to design lab-on-a-chip devices capable of performing all sample preparation and analyte detection in one miniaturized microfluidic sensor.

In addition, other nanofiber surface chemistries can be studied to create more specific sample filtration and allow for immobilization of biological recognition element.

BIOGRAPHICAL SKETCH

Originally from Colorado, Lauren is the eldest daughter of Richard and Judy Matlock. She graduated cum laude with a Bachelor of Science from Cornell University in 2009. Her research interests include microfluidics, nanofibers, and lab-on-a-chip devices. In her free time, Lauren enjoys sewing, running, and cooking.

This work is dedicated to my wonderful parents, Richard and Judy Matlock.

ACKNOWLEDGEMENTS

I would like to express my deepest appreciation to my research advisor, Dr. Antje Baeumner. I could not have completed this work without her guidance and encouragement. I am also grateful to my collaboration advisor, Dr. Margaret Frey, for her help and support throughout the course of this project. I would like to acknowledge Dr. Brian Kirby for serving on my committee and for teaching me microfluidics. I am thankful for his time, patience, and advice.

I wish to thank my collaborator, Dr. Daehwan Cho, for teaching me how to electrospin and for designing all the nanofibers used within my project. I am indebted to him for his advice and assistance with the design and execution of my experiments.

Several people contributed to the success of this project. I would like to acknowledge the Wiesner Lab at Cornell University for providing the CDots used to image our nanofibers. I would also like to thank Dr. Katie Edwards for making the liposomes used in this work.

Special thanks go to my colleagues in the Baeumner Lab. John Connelly, Christine Pitner, Sarah Reinholt, Barbara Leonard and Katie Edwards- thank you for your encouragement, advice, and lunchtime conversations.

Finally, I would like to thank the Lester B. Knight Fellowship at Cornell University and the NSF IGERT program provided through the Cornell Center for Materials Research. I am also grateful for the financial support provided by NSF CBET-0852900 and the National Textile Center. Partial funding for this research was also provided by the Cornell Agricultural Experiment Station through federal funding project 356 : " Novel Nanofiber Biosensor for Food Safety"

TABLE OF CONTENTS

LIST OF FIGURES

LIST OF TABLES

LIST OF ABBREVIATIONS

AChE	Acetylcholinesterase
BE	Binding energy
BSA	Bovine serum albumen
CA125	Carcinoma antigen 125
CDots	Cornell dots
ChOx	Cholesterol oxidase
CNF	Cornell NanoScale Science and Technology Facility
DI	Distilled
FTIR	Fourier transform infrared spectroscopy
GFE	Graphitized carbon fibers
GOx	Glucose oxidase
hMSC	Human mesenchymal stem cells
HSS	HEPES-sucrose-saline
MIPs	Molecularly imprinted polymers
NASBA	Nucleic acid sequence base amplification
NBTC	Nanobiotechnology Center
PANI	Polyaniline
Polybrene	Hexadimethrine bromide
PCR	Polymerase chain reaction
PDMS	Polydimethylsiloxane
PLA	Polylactic acid
POLY(MA)	Poly(methyl vinyl ether-alt-maleic anhydride)
PMMA	Poly(methyl methacrylate)

PPy	Polypyrrole
PVA	Poly(vinyl alcohol)
SEM	Scanning electron microscope
SPAN	Self-doped polyaniline
TRITC	Rhodamine isothiocyanate
TSC	Thermally stimulated current
μTAS	Micro-total analysis systems
UVO	Ultraviolet Ozone
VACNFs	Vertically aligned carbon nanofibers
XPS	X-ray photoelectron spectroscopy

CHAPTER 1

Recent Progress in the Design of Nanofiber-based Biosensing Devices

Abstract

This review addresses recent progress made in the use of nanofibers for analyte detection and sample preparation within analytical devices. The unique characteristics of nanofibers make them ideal for incorporation within sensors designed to allow for sensitive detection of clinical, environmental, and food safety analytes. In particular, the extremely large surface area provided by nanofiber mats and arrays drastically increases the availability of immobilization sites within biosensors. Additionally, nanofibers can be made from a variety of biocompatible materials and can be functionalized through the incorporation of nanoscale materials within spinning dopes or polymerization solutions. Finally, methods of nanofiber formation are largely well understood, allowing for controlled synthesis of nanofiber mats with specific sizes, shapes, pore sizes, and tensile strengths. In this paper, we present a survey of the different materials that are currently being used to produce nanofibers for use within sensing devices. In addition, we compare the limits of detection and linear ranges of nanofiber-based sensors and conventional sensors to determine if detection is improved by the inclusion of nanoscale materials.

1. Introduction

Materials with dimensions on the nanoscale (nanomaterials) are increasingly being integrated within analytical systems to allow for the detection of low concentrations of analytes without complicated amplification processes such as polymerase chain reaction (PCR) and nucleic acid sequence base amplification (NASBA) [4-6]. One of the main advantages of

nanomaterials is their extremely high surface area to volume ratio, which increases the number of binding sites available for biological recognition element immobilization. In addition, the use of nanomaterials can result in faster mass transfer rates, resulting in lower limits of detection and faster analyte detection rates than those seen in conventional sensors [5]. Several groups have demonstrated the successful fabrication of sensitive biosensors using one-dimensional nanostructures such as carbon nanotubes and single nanowires [7-9]. These sensors utilize the fast mass transfer and large surface areas provided by the nanomaterials, but can exhibit high background noise and variable signals [5]. In addition, the reproducible synthesis of carbon nanotubes and wires is often difficult and many fabrication processes have poor control over the size, shape and densities of the materials produced [4, 7]. Consequently, many nanomaterial-based biosensors have variable signals, making them ill-suited for commercialization. In order to address these limitations, nonwoven nanofiber mats and arrays are being examined as alternatives to one-dimensional nanostructures [5]. A unique advantage of nanofiber mats and arrays is that their entire surface area can easily be functionalized with nanoscale materials due to the presence of oxygen-containing activated sites on the nanofiber surfaces [4]. On the other hand, carbon nanotubes have a closed shell structure that limits how they can be functionalized [8]. This is due to the fact that adsorption and covalent immobilization are only possible at the open ends of nanotubes. Functionalizing the sides of carbon nanotubes is more complicated and requires oxidation and chemical modification of the nanotube walls [8].

Nanofibers can be produced by a variety of methods, including electrospinning, interfacial polymerization, and catalytic synthesis [10]. These processes are generally well-understood and allow for controlled synthesis of nanofibers with specific sizes, shapes, tensile strengths, and chemical functionalities [10, 11]. Nanofibers can also be made out of several

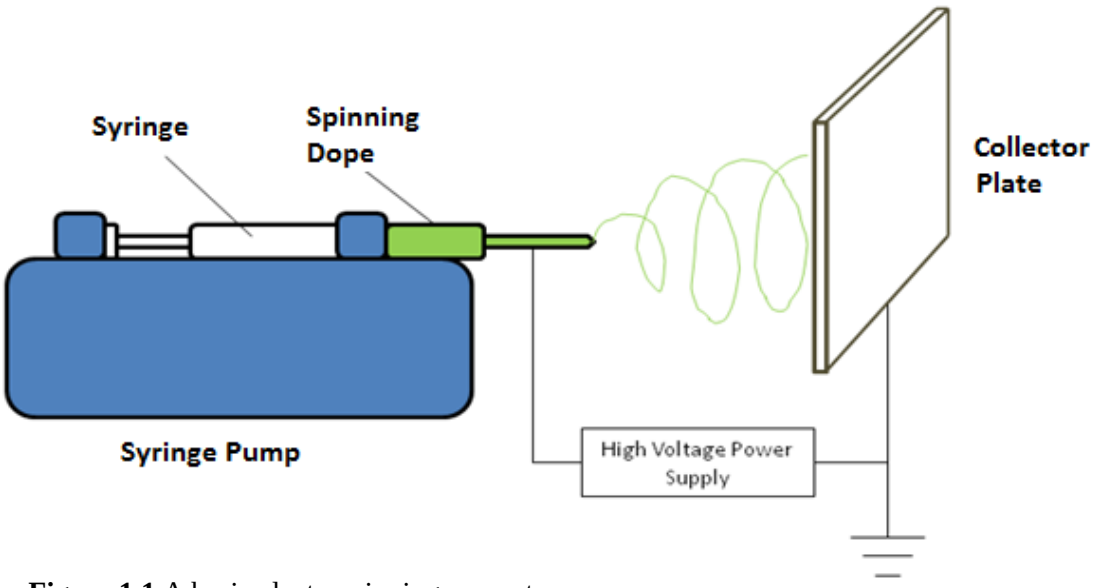

Figure 1.1 A basic electrospinning apparatus

materials that exhibit high chemical stability and biocompatibility, allowing them to be used in a variety of conditions and with a variety of analytes [12].

Electrospinning is a nanofiber synthesis method that has been used for over 75 years [13].

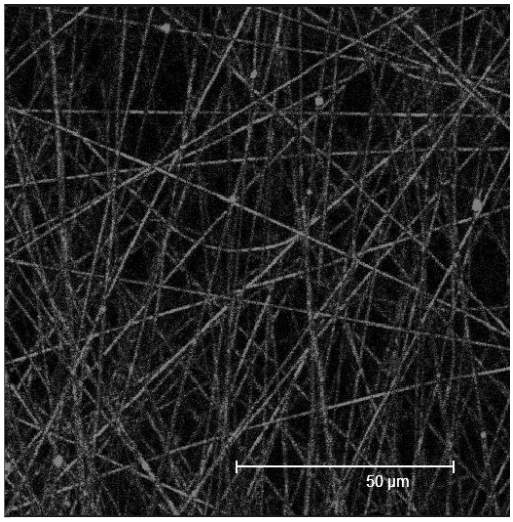

Figure 1.2 Confocal microscopy image of Poly(vinyl alcohol) electrospun nanofibers

During electrospinning, electrical forces are used to form ultrathin fibers from polymer spinning dopes [10, 11]. The fibers formed during electrospinning have diameters on the order of 100 nm, though smaller fibers can be produced [11, 14]. A typical electrospinning apparatus consists of a spinneret (typically a syringe) containing the polymer spinning dope, a pump, a high voltage source, and a grounded collector plate (Figure 1.1). During electrospinning, the pump is used to slowly push the polymer solution out of the spinneret. The tip of the spinneret is attached to a

high voltage power source in order to confer a constant charge on the polymer solution. When subjected to an electrical force, the polymer solution will form a cone, called a Taylor cone, at the tip of the spinneret [11, 15]. The electric field strength at the tip of the cone can be expressing using $E = \sqrt{\frac{4\gamma}{\varepsilon_o R}}$, where γ is the surface tension of the spinning dope, ϵ_0 is the permittivity of the free space, and R is the radius of curvature of the cone apex [16]. A grounded collector plate is placed across from the spinneret, and the polymer solution accelerates towards the collector plate when the electrostatic forces between the collector plate and the spinneret overcome the surface tension at the spinneret tip [10]. After leaving the spinneret, the polymer solution undergoes whipping, and the solvent evaporates, resulting in a solid polymer fiber [11]. The nanofibers accumulate on the collector plate, forming nonwoven mats with extremely high surface area to volume ratios and small pore sizes (Figure 1.2) [15].

Parameters that affect the spinnability of a polymer melt include spinning solution concentration, conductivity and viscosity, atmospheric temperature and humidity, feeding rate, and the distance between collector plate and spinneret [10, 15]. Many groups have investigated how these parameters affect the morphology of the nanofibers produced. Spinning dope viscosity is one of the most important parameters affecting the diameter of the nanofibers produced during electrospinning [17]. Because polymer solution viscosity is dependent on polymer concentration, the higher the polymer concentration the larger the nanofiber diameters become. Demir *et al*. have shown that a power law relationship can be used to model how fiber diameter will increase as polymer concentration is increased, with fiber diameter being proportional to the cube of the polymer concentration [18]. A higher polymer concentration has also been shown to result in less beading on the nanofiber surfaces [17]. The applied electrical voltage also has a significant effect on nanofiber diameter. A higher applied voltage causes more fluid to be ejected in a jet,

causing larger fiber diameters [18]. The polarity of the electric potential has been shown to have no effect on the spinning process, and fibers can be spun using both negative and positive potentials [16].

Electrospun nanofibers can easily be functionalized through the incorporated of nanoscale materials within the spinning dope. Conductive nanofibers are frequently fabricated by doping polymer solutions with carbon nanotubes or nanoparticles [12, 19]. Enzymes have also successfully been immobilized within nanofiber networks. Moradzadegan *et al.* created poly(vinyl alcohol) (PVA) nanofibers containing acetylcholinesterase (AChE) by electrospinning a melt of PVA, AChE, and bovine serum albumen (BSA) as an enzyme stabilizer [20]. The AChE modified nanofibers exhibited a 40% activity recovery after electrospinning. Additionally, the enzymes within the nanofibers had a higher stability in acidic solutions when compared to free enzymes. More recently, several groups have looked at the incorporation of molecularly imprinted polymers (MIPs) within nanofiber networks to construct high sensitivity analytical systems [14, 21]. Electrospun polyimide nanofibers imprinted using a diamine monomer template were able to bind and detect estrone with high sensitivity [21]. The electrospinning of molecularly imprinted nanoparticles within PVA was also able to produce nanofiber mats capable of differentiating between butoxycarbonyl -L-phenylalanine and butoxycarbonyl -D-phenylalanine [14].

Nanofibers can be fabricated through other methods, such as interfacial polymerization and catalytic synthesis [10]. The fibers produced using these techniques have lengths on the nano to micrometer scale, making them significantly shorter than electrospun nanofibers [21]. Interfacial polymerization is a non-template method of fabrication in which high local concentrations of monomers and dopant anions at a liquid-liquid interface are used to form

monomer-anion aggregates [23]. These aggregates serve as nucleation sites for polymerization, ultimately producing nanofiber networks. Interfacial polymerization is often used in the production of polyaniline fibers using organic solvents such as benzene, toluene, or carbon tetrachloride [22, 23]. Nanofiber seeding, in which small amounts of nanofibers are added to a traditional polymerization solution, has been used to increase the efficiency of nanofiber synthesis [24]. In 2004, Zhang *et al*. described a method for synthesizing polypyrrole nanofibers by seeding a polymerization solution with 1-4 mg of 15 mm diameter V_2O_5 nanofibers and noted that the nanofiber production was increased compared to interfacial polymerization methods [25]. Catalytic synthesis is commonly used to fabricate carbon nanofibers [26, 27]. Vertically aligned carbon nanofibers were synthesized by Klein *et al.* using a co-sputtered catalysis method [26]. A Cu-Ni composition gradient was used to grow the nanofibers using plasma chemical vapor etch deposition, yielding fibers with various morphologies based on the percentage of Ni used. Toebes *et al.* used a silica-supported nickel catalyst to produce fishbone carbon nanofibers [27]. The nanofibers produced had uniform morphology and 25 nm diameters.

Nanofibers are increasingly being incorporated within biosensors to improve the sensitivity and selectivity of analyte detection. This review looks at the materials most frequently used to form nanofibers for use within sensing systems. We examine the advantages and disadvantages of each material and discuss the effects of nanofiber incorporation on sample preparation and analyte detection.

2. Applications

2.1 Carbon Nanofibers

Carbon electrodes have long been used within electrochemical biosensors because they are affordable, biocompatible, and have excellent electron transfer kinetics [28, 29]. Carbon nanomaterials, specifically carbon nanotubes, have also been integrated within electrochemical sensors in order to increase the sensitivity of detection [4, 7, 8, 29-32]. In particular, carbon nanotubes offer improved electronic properties and faster electrode kinetics when compared with conventional carbon electrodes [29]. The Wang group demonstrated the first use of carbon nanotubes within biosensors by utilizing a carbon nanotube-based electrode for the detection of the reversible oxidation of dopamine [29]. More recently, single walled carbon nanotubes have been used in the design of electrodes for nucleic acids, cancer biomarkers, neurotransmitters, proteins, and glucose [7, 29]. Though carbon nanotubes have successfully been used within biosensors, their commercial viability is currently limited by the fact that their performance is highly dependent on their chirality and diameter, both of which can be difficult to precisely control during synthesis [4, 7]. In addition, functionalizing the whole surface of carbon nanotubes can be difficult. Adsorption and covalent immobilization can only be used to functionalize the ends of nanotubes, while oxidation and chemical modification are required to modify nanotube walls [8].

Due to these limitations, many labs are investigating carbon nanofibers as an alternative to carbon nanotubes for highly sensitive analyte detection. Carbon nanofibers have the same high conductivity observed in carbon nanotubes, but can provide an even larger functionalized surface area for the immobilization of biomolecules [33]. They can also be easily functionalized along their entire length due to oxygen-containing activate sites on their surfaces [4]. In general, carbon

nanofibers are cylindrical and consist of grapheme layers and typically have lengths on the order of micrometers.

Vertically aligned carbon nanofibers (VACNFs) are frequently used to create nanoelectrode arrays for analyte detection [27, 34, 35]. An advantage of these fibers is that they can be individually grown, which allows for a high level of control over the spacing and morphology of VACNF electrodes. In particular, the individual nanofibers can be spaced far enough apart to ensure that the overlapping of radial diffusion layers of adjacent fibers is prevented, but close enough to make densely packed electrode bundles [36]. VACNFs can also be individually functionalized to create heterogeneous electrode bundles [34, 35, 37, 38]. In 2004, Le *et al.* presented a method for chemically modifying densely packed VACNF electrode arrays with DNA, proteins, and antibodies [34]. Electrochemical reduction of nitro groups to amino groups on the nanofiber surfaces was used to selectively attach DNA sequences to specific fibers within a 500 nm diameter fiber bundle. Carbon nanotubes were also functionalized with a similar method, but the VACNF arrays were more densely packed. Mcknight *et al.* demonstrated a method of heterogeneous functionalization of VACNF arrays using photoresist blocking [35]. The VACNFs in this study were functionalized with gold, conductive polymers, DNA, and biotin to allow for the capture of enzyme and quantum-dot-conjugated streptavidin. Baker *et al.* developed a method of functionalizing nanofibers through reaction with liquid-phase molecules containing alkene groups [37,38]. Nanofiber arrays modified with primary amines, carboxylic acid groups and alkyl groups were developed. These arrays were successfully used to immobilize cytochrome c for a colorimetric assay [39].

In general, though vertically aligned carbon nanofibers could theoretically provide a larger functionalized surface area than carbon nanotubes, the current standard is to utilize a

matrix to immobilize VACNFs so that only their open ends are exposed on the electrode surface [36]. This immobilization serves two purposes. First, it prevents the nanofibers from collapsing upon contact with assay liquids. In addition, exposing only the VACNF ends reportedly increases the sensitivity of the sensors and reduces the occurrence of background "leakage" currents [36]. Consequently, the use of carbon nanotubes and VACNFs are not significantly different in terms of surface area and functionalization. In addition, the reproducible fabrication of VACNF arrays with uniform fiber heights and densities remains a key challenge to their widespread use, just as with carbon nanotube arrays. Several groups have demonstrated that the signals produced by nanofiber arrays are highly dependent on uniform array morphology [36, 40]. In 2009, Arumugam *et al.* attempted to limit variations in nanofiber density by using electron beam patterning on catalyst dots to produce VACNF arrays [30]. The group successfully reduced variations in fiber densities, and was able to successfully detect target DNA from *E.coli* O157:H7. However, signal variations attributed to differences in fiber heights were still observed. The group was later able to address the variations in fiber height through the development of an improved electron beam deposition procedure that allowed for the creation of a reproducible electrochemical sensor for the 16 rRNA gene from *E.coli* O157:H7 [40]. Despite these advances, several improvements to VACNF electrode design need to be made before they can outperform carbon nanotubes and be used in commercial devices, including improvements to material preparation, probe chemistry, and signal transduction [40].

More often described is the use of carbon nanofiber mats to modify electrodes for use with electrochemical biosensors [4, 33, 47] similar to other chemical and polymer modifications frequently used in electrochemistry [41]. These nanofiber films increase the surface functionality of the electrodes and can increase the sensitivity of detection for a variety of different analytes

without increasing biosensor size [33, 42, 43, 47]. Glucose oxidase has been successfully immobilized on carbon nanofiber-modified electrodes to produce high sensitivity glucose biosensors [4, 44]. In 2006, Vamvakaki examined different types of carbon nanofibers to determine which were most appropriate for glucose biosensing systems [4]. Their research indicated that graphitized carbon fibers (GFE) had exceptional enzyme loading properties and remarkable stability. The GFE fibers were produced by heat treating basic carbon nanofibers at 3000 ºC and consist of graphene layers arranged in a reversed saw-tooth morphology. The nanofibers were modified with glucose oxidase and maintained their initial activity after 100 hours of continuous operation.

When used to modify an electrode, the larger functional surface area of carbon nanofibers can be taken advantage of and improve performance when compared with carbon nanotubes. Wu *et al.* created an electrochemical glucose sensor using carbon nanofibers modified with glucose oxidase and nafion [44]. The immobilization of oxygen-containing groups on the surface of carbon nanofibers was compared to the immobilization of the same groups on carbon nanotubes and the authors report that there were twice as many functional groups on the fibers than on the nanotubes [44]. The sensor had a liner range of 10-350 μM and a limit of detection of 2.5 μM. Its sensitivity was five times higher than many previously reported glucose sensors, including a similar glucose oxidase/titania sol-gel sensor, which had a limit of detection of 70 μM [46]. In addition, the sensor was resistant to interference from a clinically relevant concentration of ascorbic acid (0.08 mM). The concentration of uric acid in human serum samples is generally between 0.18-0.42 mM [45]. Therefore, though the carbon nanofiber sensor was not affected by the interference of 0.08 mM of uric acid, a higher concentration needs to be tested to be truly

clinically relevant. However, the sensitivity and stability of the glucose sensor is promising for detection of glucose in clinical samples.

In 2009, Zhang *et al.* reported an amperometric sensor for phenol detection using a polyaniline-ionic liquid carbon nanofiber composite [47]. The composite was formed through electropolymerization of aniline and carbon nanofibers in an ionic liquid. The polyaniline was shown to grow along the carbon nanofibers, resulting in a composite film with fibrillar morphology (95 nm diameter). The composite was used to modify a glassy carbon electrode and was functionalized through the immobilization of tyrosinase on the nanofiber surfaces. The high surface area of the nanofiber film showed a higher tyrosinase immobilization capacity than previously reported devices. The biosensor had a large linear response to catechol detection, ranging from 4.0×10^{-10} to 2.1×10^{-6} M and a limit of detection of 0.1 nM, making it more sensitive than other catechol sensors that do not employ nanofiber mats [48]. The sensor was unaffected by interference from 3 µM ascorbic acid, 30 µM uric acid, and 30 µM caffeine, which is promising for phenol detection in real samples.

Thionine-carbon nanofibers have been used to create an amperometric ethanol sensor [33]. Electrochemical polymerization was used to form a thionine/carbon nanofiber composite on an electrode surface. The nanofiber film was functionalized with alcohol oxidase and was used to detect ethanol through the reduction of dissolved oxygen. The sensor had a limit of detection of 1.7 µM, which is significantly lower than the 6.26 mM observed in alcohol oxidase immobilization in electrochemically deposited resydrol films [33].

Wu *et al*. have reported an amperometric immunosensor for the detection of carcinoma antigen 125 (CA125) using horseradish peroxidase-labeled carbon nanofibers [42]. The

immobilized horseradish peroxidase exhibited good enzymatic activity towards the oxidation of thionine by hydrogen peroxide. The nanofiber-modified biosensor did not require an electron transfer mediator and therefore required fewer incubation and washing steps than conventional CA125 sensors. The device was used to successfully detect CA125 in standard solutions with a large linear range (2-75 U/mL) when compared with previously developed sensors, and a detection limit of 1.8 U/mL [47]. CA125 detection in serum samples was also carried out and demonstrated comparable results with a commercial electrochemiluminescent assay.

Carbon nanofibers have successfully been used within electrochemical biosensors for a variety of analytes. Vertically aligned carbon nanofibers, which can serve as bundles of nanoelectrodes, have been shown to increase the sensitivity of analyte detection when compared with biosensors that do not utilize nanomaterials. However, they are currently plagued by the same variable synthesis as carbon nanotubes. In addition, the current method of exposing only the tops of VACNFs fails to take advantage of the high functionalizable surface areas of nanofibers. Carbon nanofibers have also been used to increase the surface area and functionality of electrodes. In these applications, nanofibers have successfully been used to increase the number of functional sites when compared to nanotubes or non nanoscale materials. Biosensors utilizing carbon nanofibers improved the sensitivity of biosensors for glucose, catechol, and ethanol. In addition, the nanofibers dramatically increased the linear range for CA125 detection (Table 1.1).

Table 1.1 Comparison of linear range and limit of detection for nanofiber-based and conventional biosensors

Sensor Materials	**Analyte**	**Linear Range**	**Limit of Detection**	**Reference**
Carbon Nanofibers	Glucose	10-350 μM	2.5 μM	Wu *et al.* 2007 [44]
GOx/titania sol-gel	Glucose	70-15,000 μM	70 μM	Yu *et al.* 2003 [46]
Polyaniline/carbon nanofiber composite	Catechol	4.0×10^{-4} – 2.1 μM	0.0001 μM	Zhange *et al.* 2009 [47]
Polyaniline/polyphenol oxidase film	Catechol	2.5 -140 μM	0.05 μM	Tan *et al.* 2011 [48]
Thionine/carbon nanofibers	Ethanol	2.0 – 252 μM	1.7 μM	Wu *et al.* 2007 [33]
Resydrol film	Ethanol	Not reported	6,260 μM	Lyudmyla *et al.* 2006 [49]
Peroxidase-labeled carbon nanofibers	CA125	2-75 Units/mL	1.8 Units/mL	Wu *et al.* 2007 [42]
Peroxidase film	CA125	2-14 Units/mL	1.29 Units/mL	Dai *et al.* 2003 [50]

2.2 Polyaniline Nanofibers

Conductive polymers, like polyaniline (PANI), are frequently used as immobilization matrices for enzymes within electrochemical biosensors [51].The PANI matrix provides a porous medium for immobilization and facilitates electron transfer between enzymes and electrodes. PANI nanostructures have also been successfully utilized in electrochemical biosensors [52].

Berti *et al.* utilized PANI nanotubes to modify an electrode surface through electrochemical polymerization with alumina nanoporous membranes as a mold. These nanostructures were grafted with molecularly imprinted polymer receptors to create a catechol biosensor [52]. Nano-structured polyaniline films have also successfully been used to immobilize glucose oxidase to facilitate electrochemical detection [53].

Polyaniline nanofibers are also frequently used to increase the sensitivity and conductivity of electrochemical biosensors [54-53]. Compared to conventional PANI materials, PANI nanofibers have the advantage of being inexpensive, easy to produce, and have a much larger surface area [54]. However, PANI's redox activity is generally restricted to acidic environments, limiting its use in biological systems, which frequently are neutral pH environments [55]. Therefore, self-doped polyaniline (SPAN) is also utilized within nanofibers. SPAN is produced through copolymerization of aniline and m-aminobenzenesulfonic acid in an aqueous solution and features better activity and stability at neutral pH [56, 58]. Additionally, SPAN is more hydrophilic than polyaniline and can be easily functionalized with oxygen-containing groups [58].

Polyaniline nanofibers are often used to modify glassy carbon electrodes for enzyme immobilization because of their conductivity and electroactivity. In particular, hydrogen peroxide sensors utilizing PANI nanofibers have recently gained significant attention. In 2009, Du *et al.* described a simple electrode modification method in which a mixture of PANI/chitosan nanofibers and horseradish peroxidase were dropped onto a glassy carbon electrode to produce a hydrogen peroxide biosensor [54]. The nanofibers were fabricated using interfacial polymerization with 4-toluenesulfonic acid as a dopant. The PANI nanofibers were dispersed in a chitosan solution to improve nanofiber stability. The immobilized horseradish peroxidase was

shown to keep its native activity and successfully reduced H_2O_2. The device had a wide linear range of 1 x 10^{-5} to 1.5 x 10^{-3}M and a low limit of detection of 5 x 10^{-7} M. Recently, Chen *et al.* incorporated gold nanoparticles within SPAN nanofibers and immobilized horseradish peroxidase on the nanofiber surfaces to create a sensitive H_2O_2 sensor [56]. The gold nanoparticles served to increase the conductivity and biocompatibility of the SPAN nanofibers. The increased number of enzyme immobilization sites resulted in increased electrocatalytic activity in the reduction of H_2O_2 in the presence of hydroquinone. The sensor was used for successful detection of H_2O_2 in real contact lens solution samples and results were comparable to those obtained by conventional potassium permanganate titration. These two PANI nanofiber biosensors allowed for sensitive detection of hydrogen peroxide, but their performance was not better than a similar PANI/nanotube sensor (table 1.2). However, when compared to a sensor composed of a thin polyaniline film on a platinum disc electrode, the PANI nanofiber sensors had a dramatically lower limit of detection [59]. This demonstrates the benefits of the larger surface area provided by nanomaterials such as nanofibers and nanotubes.

Polyaniline nanofibers have also been used to increase the sensitivity of DNA detection [6, 55, 57]. In 2011, Wang *et al.* utilized three-step electrodeposition to create self-doped polyaniline nanofibers patterned with Au microspheres [55]. The nanofibers were used to modify a glassy carbon electrode in order to detect a gene fragment from the cauliflower mosaic virus 255 gene. The limit of detection observed (1.9 x 10^{-14} M) was lower than previously reported non-nanofiber based DNA sensors [61]. ZrO_2 microparticles have also been used to create SPAN nanofiber membranes for DNA sensing on glassy carbon electrodes [57]. An ssDNA sequence was immobilized to the ZrO_2/SPAN/electrode surface to allow for the detection of target DNA.

Table 1.2 Comparison of PANI sensors for hydrogen peroxide

Sensor Materials	**Analyte**	**Linear Range**	**Limit of Detection**	**Reference**
Polyaniline nanofiber/chitosan film	Hydrogen Peroxide	10 - 1500 μM	0.5 μM	Du *et al.* 2009 [54]
Polyaniline nanotube/chitosan nanocomposite	Hydrogen Peroxide	1.0 – 2200 μM	0.5 μM	Wang *et al.* 2009 [60]
Gold nanoparticle/SPAN nanofiber	Hydrogen Peroxide	10 – 2000 μM	1.6 μM	Chen *et al.* 2011 [56]
Polyaniline film	Hydrogen Peroxide	250 – 5,000 μM	250 μM	Mathebe *et al.* 2004 [59]

The ZrO_2 microparticles have a high affinity for the oxygen containing groups on the nanofibers and therefore could be electrochemically deposited on nanofiber surfaces using cyclic voltammetry. The sensor also demonstrated a very low limit of detection (3.4×10^{-13} M) and specificity for target DNA and did not detect one base pair mismatch DNA sequences or non-complementary DNA. Spain *et al*. also demonstrated DNA detection using PANI nanofibers modified with gold nanoparticles on a gold electrode surface [6]. This device utilized the enzyme immobilization properties of PANI to immobilize horseradish peroxidase on the surface of the nanofibers. The nanoparticles were used to immobilize ssDNA complementary to a target strand of DNA from *Staphylococus aureus*. Hybridized target DNA was detected using the reduction of hydroquinone to mediate electron transfer to bound horseradish peroxidase. The device was able to successfully differentiate between *S. aureus* and *S. epidermis*, indicating a low false positive

rate that makes it a promising option for detection in real samples. In addition, the sensitivity of detection was 40-fold greater than detection using a bare electrode surface [6].

The successful incorporation of PANI and SPAN nanofibers within DNA sensors shows great promise for the development of highly sensitive genetic sensing. The increased surface area provided by the nanofibers resulted in a dramatic increase in the linear range when compared to non-nanofiber based sensors (Table 1.3). In addition, the limits of detection for PANI and SPAN nanofiber sensors were significantly lower than their conventional counterparts.

Table 1.3 Comparison of polyaniline nanofiber and polyaniline matrix DNA biosensors

Sensor Materials	**Analyte**	**Linear Range**	**Limit of Detection**	**Reference**
SPAN nanofiber/ Au microscphere	Cauliflower mosaic virus	1.0×10^{-7} – 1.0 μM	1.9×10^{-8} μM	Wang *et al.* 2011 [55]
Nanogold-modified poly-2,6-pyridinedicarboxylic acid film	PAT gene fragment	1.0 x 1-$^{-4}$ – 0.1 μM	2.4×10^{-5} μM	Yang *et al*. 2007 [61]
ZrO_2/SPAN nanofiber/carbon electrode	ssDNA	1.0×10^{-6} – 1.0 μM	3.4×10^{-7} μM	Yang *et al.* 2011 [57]
Au nanoparticle/polyaniline nanofiber	*S. aureus*	150×10^{-6} – 1 μM	pM range	Spain *et al.* 2010 [6]

2.3 Chitin/Chitosan Nanofibers

Chitin, and its derivative chitosan, are biodegradable and biocompatible polymers derived from the exoskeletons of arthropods and the cell walls of yeast and fungi [62, 663]. Chitosan is an excellent substrate for enzyme immobilization and can easily be electrospun into high surface area nanofiber mats. In addition, chitosan nanofibers exhibit high mechanical strength, hydrophilicity, and exceptionally small pores size when spun into mats [62]. Chitin, on the other hand, is a difficult material to work with and does not dissolve in most common solvents. However, both chitin and chitosan nanofibers have been successfully used in many applications, such as drug release, tissue engineering, and wound healing [63]. Chitosan has traditionally been used to immobilize enzymes within biosensors due to the amino group and two hydroxyl groups in each molecular unit that can easily be crosslinked within different substances [64, 65]. Chitosan/$NiFe_2O_4$ nanoparticles have also been used to immobilize glucose oxidase for electrochemical detection in a glassy carbon electrode biosensor [66]. Finally, three-dimensional chitosan membranes have also been utilized to increase electrode surface areas for electrochemical detection [67].

Recently, chitin and chitosan nanofibers have been incorporated within biosensing devices to take advantage of their excellent enzyme immobilization properties. An amperometric cholesterol biosensor consisting of cholesterol oxidase (ChOx) immobilized on a chitosan nanofiber/gold nanoparticle network has been developed by Gomathi *et al.* The nanofibers had diameters ranging from 50-100 nm and were prepared by oil/water emulsion [62]. The gold nanoparticles were electrochemically deposited on the nanofibers from a $HAuCl_4$ solution. The device was able to reproducibly measure cholesterol within real human serum samples and did not respond to clinically relevant concentrations of ascorbic acid and uric acid in PBS [62]. The

limit of detection (0.5 μM) was also substantially lower than the limit of detection observed in non-nanofiber based sensors (Table 1.4) [68]. Chitosan/poly(vinyl alcohol) electrospun nanofibers have also been used for enzyme immobilization within biosensors [69]. The nanofibers had diameters ranging from 80-150 nm and were utilized for enzyme immobilization due to their biocompatibility and porosity. The enzymes were used to immobilize lipase from *Candida rugosa* using glutaraldehyde as a coupling reagent. The immobilized enzyme retained 49.8% of its activity and had improved thermal and pH stability when compared to free enzyme.

Table 1.4 A comparison of chitosan nanofiber and chitosan film cholesterol biosensors

Sensor Materials	**Analyte**	**Linear Range**	**Limit of Detection**	**Reference**
Chitosan nanofiber/gold nanoparticles	Cholesterol	1-45 μM	0.5 μM	Gomathi *et al.* 2011 [62]
Metal oxide/chitosan composite film	Cholesterol	100-400 mg/dL	5 mg/dL	Malhotra *et al.* 2009 [68]

2.4 Poly(vinyl alcohol) Nanofibers

Poly(vinyl alcohol) (PVA) is a water-soluble, biocompatible polymer that has excellent fiber formation properties [70]. Unlike many other polymers, PVA has the advantage of being able to be electrospun using water as a solvent and can be easily stabilized through cross-linking of the free-hydroxyl groups on the fiber surfaces [14]. The hydroxyl groups can also be used to easily functionalize the nanofibers. Generally, PVA membranes have been used to immobilize enzymes within electrochemical biosensors [71]. In addition, PVA has been used to modify

carbon nanotubes for application within electrochemical biosensors [72]. The PVA serves as a binder that permits immobilization of biomolecules on the nanotube surfaces [72].

PVA nanofibers have been used as supports for molecularly imprinted polymer (MIP) nanoparticles for the detection of dansyl-L-phenylalanine [14]. Molecularly imprinted polymers are traditionally immobilized onto solid surfaces, which results in low surface areas and binding capacities. Therefore, nanofiber mats have been investigated to create a higher surface area for analyte detection. The MIPs had a diameter of 400 nm and were contained within nanofibers with diameters between 80-350 nm to ensure that the binding sites of the nanoparticles were not completely covered by the fibers. Fluorescent microscopy confirmed the binding of dansyl-L-phenylalanine to the MIPs with no nonspecific binding of the analyte to the fibers.

PVA nanofibers have also been used for enzyme immobilization in amperometric biosensors [73]. The nanofibers were used to immobilize glucose oxidase to allow for the sensitive detection of glucose. Chronoamperometric measurements showed that the nanofiber modified electrodes demonstrated a rapid response (1 second) and had a good detection response (μA level) to both normal and diabetic levels of glucose. The device had a linear range from 1-10 mM and a detection limit of 0.05 mM. This limit of detection is lower than the limits of detection observed in some non-nanofiber sensors [45], but is higher than carbon-nanofiber sensors that have been developed [44].

Recently, Cho *et al.* demonstrated the successful incorporation of electrospun PVA nanofibers within microfluidic systems to allow for sample preparation as well as analyte detection within microfluidic devices [74]. Positively charged PVA fibers were fabricated through the incorporation of hexadimethrine bromide within the polymer spinning dope, while

negatively charged fibers were produced using poly(maleic anhydride). These fibers were spun on gold microelectrodes patterned on poly(methyl methacrylate) and incorporated into microfluidic devices. The fibers were shown to maintain their morphology in fluid flow up to 20 µL/min. Positively charged nanofibers were shown to successfully filter negatively charged nanoparticles out of a buffer solution, allowing for sample concentration and purification within a microchannel.

2.5 Other Materials

Polylactic acid (PLA) is commonly used in the electrospinning of nanofibers for a variety of applications from tissue engineering to drug delivery [75]. In 2006, Li *et al.* utilized electrospinning to produce biotinylated nanofiber membranes that provided an extremely large number of binding sites for streptavidin [75]. Nanofibers were produced by dispersing biotin in a PLA/chloroform/acetone solution before electrospinning. Electron probe microanalysis confirmed the presence of biotin on the surface of the electrospun fibers. Additional analysis confirmed that biotin was fixed to the fiber surfaces and was not washed off during fluid flow. A basic biosensor was constructed using the nanofiber membrane to immobilize biotinylated nucleic acid probes for detecting synthetic *E.coli* DNA [75, 76].

Polypyrrole (PPy), like polyaniline, is a naturally conducting polymer, and has been used within electrochemical DNA sensors [77]. Unlike polyaniline, PPy can be synthesized using neutral pH aqueous solutions. The polymer nanofibers were grown on platinum electrodes and were synthesized through electropolymerization of pyrrole using pulse voltammetry. The device was used to detect low concentrations of spermidine with a limit of detection of 0.02 µM. Polypyrrole nanofibers have also been used to modify electrodes for the detection of salicylic

acid and aspirin [78]. Double stranded calf thymus DNA was physisorbed onto PPy nanofibers on a platinum electrode. The device showed a limit of detection of 8.26×10^{-1} and 5.24×10^{-6} μM for salicylic acid and aspirin respectively.

3. Summary

The high surface area provided by nanofiber arrays and mats has been shown to dramatically increase the sensitivity of many biosensors. Carbon and polyaniline have gained the most attention due to their conductivity, biocompatibility, and long history of use within biosensors. However, many other materials, such as polypyrrole and chitosan, have been successfully used to form nanofibers for improved detection for a wide variety of analytes.

Vertically aligned carbon nanofibers have been shown to increase the sensitivity of electrochemical biosensors. Moreover, several labs have demonstrated the ability to functionalize individual nanofibers within a VACNF bundle, allowing for the creation of heterogeneous nanofiber electrodes. Currently, VACNFs are immobilized within a matrix that serves as a support and reduces the background signals observed within the sensors. However, as only the tops of the nanofibers are available for interaction with the analyte, there is no increase in functional surface area when compared to carbon nanotubes or other nanomaterials. In addition, the reproducible synthesis of VACNF bundles can be difficult, resulting in variations in signal from sensor to sensors. Consequently, improvements to material synthesis and fiber morphology should be completed to standardize sensor behavior.

Carbon, polyaniline, chitosan, poly(vinyl alcohol), polypyrrole and polylactic acid nanofibers have also been used to increase the surface area of electrodes within electrochemical sensors. The fibers have been shown to significantly increase the available functionalized surface

area on the electrode and can result in larger linear ranges and lower limits of detection when compared to other sensors. Novel nanofiber-based biosensors are continually being reported in the literature, though generally the ability of these sensors to detect analytes within real clinical, environmental, and food safety samples is not significantly discussed. Further studies on sample preparation and analyte detection within nanofiber-based biosensors need to be conducted before they can be used in commercial sensors.

CHAPTER 2

Electrospun Nanofibers for Microfluidic Analytical Systems

Abstract

Nanofibers embedded with the functional polymers exhibited a charged surface. These fibers were incorporated into microfluidic channels to provide high surface area and functional surfaces within a microfluidic system. The positively or negatively charged nanofibers were fabricated by blending of hydrophilic PVA with functional polymers with available amine groups or carboxyl groups, respectively. X-ray photoelectron spectroscopy (XPS) and Fourier transform infrared spectroscopy (FTIR) were used to confirm the presence and location of blend components in the spun fibers. Thermally stimulated current (TSC) measurements confirmed that surface-charged nanofibers showed positive or negative currents according to the functional polymers embedded with the PVA polymer. The surface-charged nanofibers were incorporated into microfluidic channels. Poly(vinyl alcohol) (PVA) blend nanofibers formulated to create variations in fiber surface chemistry were electrospun to form patterns around gold microelectrodes on a poly(methyl methacrylate) (PMMA) chip surface. These nanofiber patterns were integrated into polymer-based microfluidic channels to create a functionalized microfluidic system with potential applications in bioanalysis. Spinning conditions and microelectrodes were optimized to enable an alignment of the nanofibers across the microfluidic channel. Importantly, nanofibers within the assembled microfluidic channels were robust and did not break or wash out of the channel under extreme fluid flow conditions at linear velocities up to 13.6 mm/s.

1. Introduction

In the area of bio-analytical sensors, detection systems have been miniaturized to take advantage of small feature sizes with low fluid consumption, faster analysis, and easy portability [1, 79]. Lab-on-a-chip devices integrate sample preparation and detection steps into one system and are applied in many clinical, environmental and food safety related industries [80]. Continuous improvement and research is being carried out not only in the improvement of biosensors but also of the sample preparation steps [81]. Separately, the capabilities of nanofibers as selective filter media [82, 83] and for specific capture of analytes from fluids [75, 84] has been demonstrated. Nanofibers can be electrospun with a broad range of chemically [85, 86] and biologically [17-89] active surfaces potentially useful in separation and capture of target analytes. Nanofibers have also been utilized to improve targeted properties in such application areas as tissue engineering scaffolding [90-92], nanofibrous membrane biosensors [75, 93], and electronic sensors [94, 95]. The nanofibers for these applications have been fabricated by electrospinning, a technique through which fibers of a range of diameters from micrometers to nanometers can be produced from an electrically driven jet of polymeric fluid [96].

Some preliminary efforts to combine micro fluidics and nanofibers have been made. Yang and Dong have demonstrated fabrication of patterned electrospun elements on glass substrates including methods for making aligned fibers or arranging fibers patches with specific size and shape by selectively etching fibers [97]. Polylactic acid and polyethylene oxide fibers were used to demonstrate the technique for patterning fibers onto glass substrates, but biocompatibility and function within a microfluidic device were not demonstrated. A detailed study of nanofiber behavior during low Reynolds number flows in microfluidic channels confirmed that fiber do not

fold or buckle within the channels under these conditions [98]. In this study, nanofibers were floating freely within the nanofiber channels. Applications for nanofibers within microfluidic devices to date have taken advantage of nanofiber arrays as scaffolds for cell growth within biological simulation devices and the selective filtration capabilities of nanofibers. Lee *et al.* incorporated a patch of randomly oriented polyurethane nanofibers into a microfluidic channel. The nanofibers were used as a synthetic extracellular matrix for growth of human mesenchymal stem cells **(**hMSC) within the channel of a bio-MEMS device. The surface properties, in particular the hydrophilicity, of the polyurethane required modification for successful cell proliferation. With this microfluidic construct (hMSC grown on a synthetic ECM within a channel), various nutrients could be provided via flow through the channel and influence on hMSC functions studied [99]. Lee et al. created a microfluidic dialysis device by a) electrospinning a non-woven filter fabric, b) making a PDMS microfluidic device, top and bottom containing a serpentine etched channel and c) sandwiching the electrospun fabric between the top and bottom of the microfluidic device [100]. As a prototype device, the preliminary dialysis results were as good as or better than currently available systems.

In the biomolecular detection process, surface-charged nanofibers can be an easy alternative to modifying the surface of a nanofiber with probe biomolecules. Surface-charged nanofibers can concentrate target biomolecules via electostatic attraction between charges on the nanofiber surface and the counter charge of the target material, thus improving detection sensitivity. As a step towards constructing a biocompatible surface for endothelial cells, Ma et al. developed an electrospun fiber mat with covalently grafted gelatin to mimic the fibrous proteins in a native extracellular matrix [101]. The charge storage performance for electrospun fiber mats was studied to characterize the surface charging potential of the ideal candidates for filter and sensing

applications [102-104]. Terada et al. introduced amino groups into polymer chains grafted onto a polyethylene membrane to evaluate the effects of surface properties on the adhesion and viability of a strain of negative and positive bacterium [105]. In addition, Ma et al. developed an affinity membrane to permit the purification of molecules based on their physical/chemical properties by immobilizing specific ligands onto the membrane surface [106].

In this study, new surface functional nanofibers were developed, incorporated into microfluidic channels and the durability of those fibers within the channels proven. Gold electrodes were patterned adjacent to the microfluidic channels to control for the positioning of the nanofibers across the channels. Nanofibers used in this study were designed to be hydrophilic with either partial positive (δ^+) or partial negative (δ^-) charge at the fiber surface under flow conditions in the microfluidic channel. The phenomenon of a formation of charged surfaces at the interface between a solid and an electrolyte is well-known [107]. These charges arise either from surface ionization (group dissociation) or ion adsorption. Our main interest in this study was to develop hydrophilic fibers with charged surfaces suitable for bio-applications. Highly hydrolyzed PVA polymers (> 99%) were blended with functional polymers targeted to provide a polarizable surface. PVA is especially useful for the materials in the bio-analysis system because it can be processed from hot water eliminating risk that the fabricated PVA nanofiber webs contain any toxic solvents which might interfere with analytes in solution. The resulting electrospun nanofibers are stabilized by strong inter-molecular hydrogen bonding [108] and do not swell significantly or dissolve in the room temperature aqueous solutions used for bioanalysis. Two types of functional polymers, Hexadimethrine bromide (Polybrene, PB) and Poly(methyl vinyl ether-alt-maleic anhydride) (Poly(MVE/MA), POLY(MA)), which have positive and negative functional groups, were blended with PVA in the electrospinning dope to

provide additional functionality. The amine groups or carboxyl groups in the functional polymers can be protonated or deprotonated in the pH of the solutions. The protonation or deprotonation of the functional polymers usually results in positive or negative charges on the fiber surface, incorporating the functional polymers. The charged surfaces on the electrospun fibers were induced when they met with the aqueous solutions due to the dissociation (ionization) of the functional groups on the surface or the adsorption (protonation) of ions from the solutions. XPS and FTIR were employed to detect and characterize the incorporation of PB and POLY(MA) in the electrospun fibers. Nanofiber alignment within the microfluidic channels was easily controlled during the spinning process and was not disrupted by the assembly of the full microfluidic device. Nanofiber stability in the microfluidic channels before and after high rates of fluid flow was evaluated by regular light microscopy. The effluent was collected from the microfluidic channels and analyzed using FTIR and H-NMR to confirm nanofiber durability. The current of the ionic blend nanofibers was measured by a thermally stimulated current (TSC) experiment [107].

The fabrication of the microfluidic channel incorporated with the charged nanofibers is aimed at the concentration or purification of target substances from a solution. Incorporation of nanofibers into microfluidic channels can add significant surface area and functionality for separation of a target analyte from a mixed fluid.

2. Experimental section

2.1. Materials

PVA polymer was purchased from Polysciences, Inc. (Warrington, PA, USA). This polymer, with a molecular weight of 78,000, is 99.7% hydrolyzed to obtain the same number of corresponding hydroxyl groups as the degree of polymerization. The functional polymers, whose

charges would be activated with ions in the aqueous solutions, were purchased from Sigma-Aldrich. The positively charged PB is soluble in water, and its molecular weight is 4,000~6,000. The negatively charged POLY(MA) is also soluble upon hydrolysis, and its molecular weight is 216,000. To reduce the surface tension of water and to retard the gelation of PVA in the spinning dope, adding a nonionic surfactant to the spinning dope is recommended [110]. Nonionic surfactant Triton X-100 (p-tertiary-octylphenoxy polyethyl alcohol) was purchased from Sigma Aldrich Company. Distilled (DI) water was used as a solvent to dissolve both PVA polymers and functional polymers.

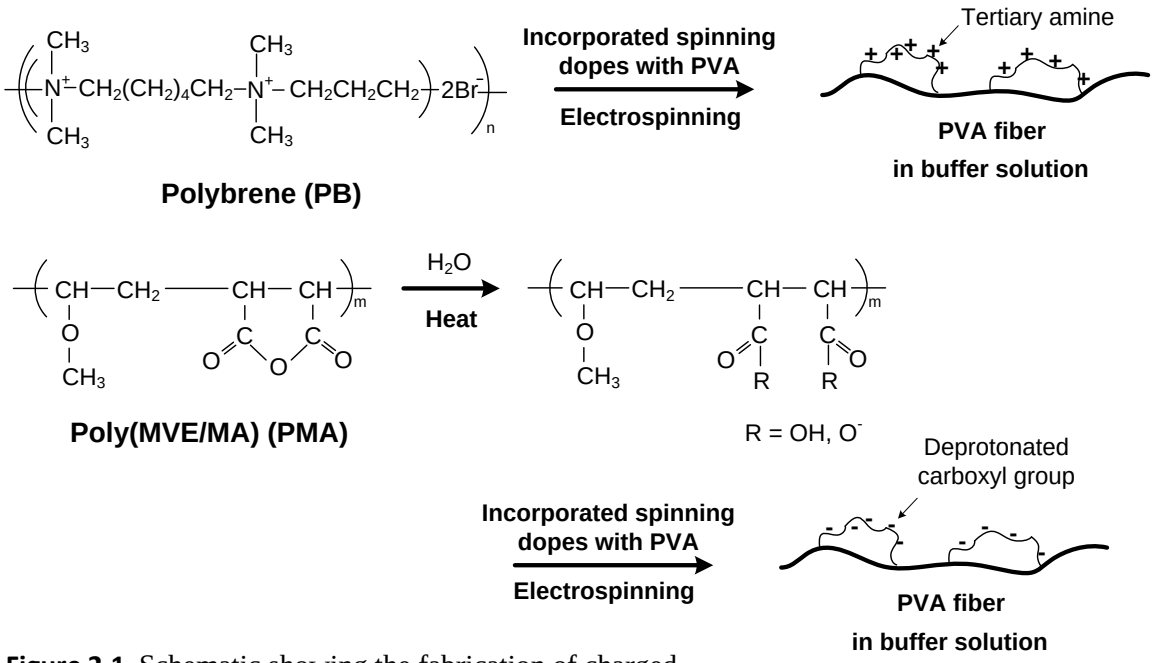

Figure 2.1 Schematic showing the fabrication of charged electrospun nanofibers

2.2. Preparation of electrospinning dopes

Two types of polymers, the PVA and the additive polymer, were used for aqueous conjugated solutions to prepare the spinning dopes. PB or POLY(MA) polymers were utilized as additive polymers to fabricate positively and negatively charged nanofibers. All procedures for

preparing the spinning dopes are described as follows. At first, 10 wt% PVA polymers were dissolved in DI water at an oven temperature of 95^{o}C for four hours. PB polymers were also dissolved in DI water at room temperature and added to the cooled PVA solution to form a solution containing PVA/PB = 90/10 wt/wt and then mixed together with a vortex for two minutes. Finally, Triton X-100 was added to the mixture solution (DI water/Triton X-100 = 99.5/0.5 wt/wt%) and agitated with a vortex for two minutes and Arm-Shaker for one hour to make a homogenous spinning dope for electrospinning positively charged nanofibers. POLY(MA) was used to fabricate the negatively charged nanofibers.

The maleic anhydride groups in POLY(MA) are derivatives of carboxylic acids, as shown in Figure 2.1. By hydrolyzing the maleic anhydride, which is treated in DI water at 90^{o}C for 15 minutes, POLY(MA) can be dissolved in water. As stated earlier, all the procedures for forming spinning dopes and spinning the fibers using POLY(MA) are the same as for PB. Polymer compositions of typical spinning dopes (without water) were; PVA/triton X-100: 89/11, PVA/PB/triton X-100: 82/8/10, PVA/POLY(MA)/triton X-100: 82/8/10.

2.3. Fabrication of nanofibrous webs

A 5 mL plastic syringe with an 18 gauge needle (inner diameter: 0.84 mm) was loaded with the prepared dope. A high voltage power supply (Gamma High Voltage Research Inc., FL) was used to apply a positive charge to the needle. To collect the electrospun fiber webs, either a grounded copper plate covered by aluminum foil or a grounded chip with electrodes was used. A micropump (Harvard Apparatus, Holliston, MA) was used to infuse the solution and to eject it toward to the collector. A voltage of 12kV was maintained at the tip of the needle. The distance between the collector and the needle tip was set at 10~15 cm, and a constant flow rate for the solution was set to 0.54 ml/hour. Electrospinning was maintained at room temperature.

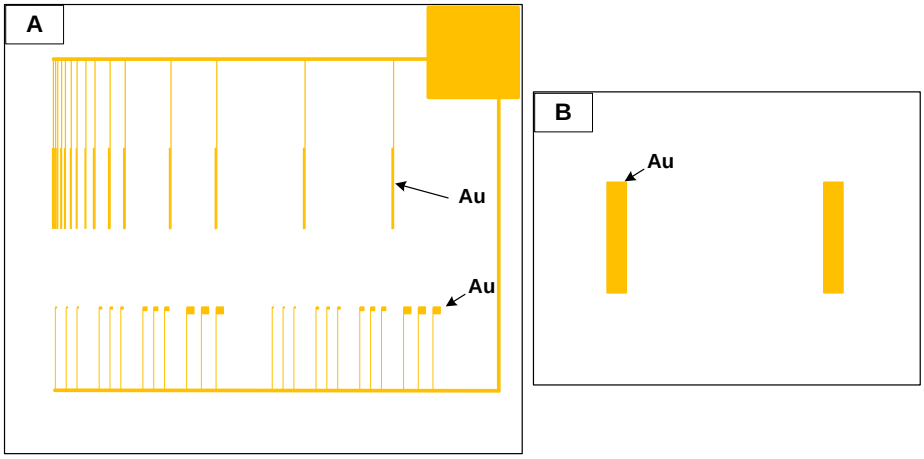

Figure 2.2 PMMA electrode chip showing a variety of sizes in electrode gaps and squares (A) and a long gap between two electrodes (B).

2.4. Fabrication of electrode chip and microfluidic channel

In a procedure carried out in the CNF (Cornell NanoScale Science and Technology Facility) as well as NBTC (Nanobiotechnology Center) at Cornell University, electrode arrays were prepared on PMMA to fabricate patterned nanofibers for incorporation in a microfluidic channel. A process for patterning Au electrodes on PMMA using gold-thiol chemistry has been described previously [111], but the use of a Cr adhesion layer was employed here instead. PMMA surfaces were cleaned by sonication for 5 minutes in 2-propanol and treated with UV light. A CHA Mark 50 evaporator (CHA Industries, Freemont, CA) was used to coat the PMMA with 10 nm Cr followed by 200 nm Au at deposition rates of 0.1 nm/s and 0.25 nm/s, respectively. A positive photoresist (Shipley 1813, Shipley, MA, USA) was then spun on the gold-coated PMMA at 3000 rpm for 30 seconds. The photoresist was UV exposed for 11 seconds through a mask containing the electrode pattern using a contact aligner (ABM, Scotts Valley, CA) and developed for one minute in MF-321 developer (Shipley Co., Marlborough, MA). The exposed Au was then etched

away by Au etchant type TFA (Transene, Danvers, MA) for one minute and the underlying Cr layer was etched away by Cr etchant (Cyantek, Freemont, CA) for 15 seconds to form the electrodes. Lastly, 100 mM NaOH was used to remove the photoresist from the electrodes. As shown in Figure 2.2 A, the electrodes were designed with varying gaps between neighboring electrodes. The following feature sizes were studied: gap size (0.1, 0.2, 0.3, 0.5, 1, 5, 10 mm) and square size (50, 100, 250, 500 μm). All the electrodes had a width of 100 μm and were connected to the corner square with 100 μm leads. The height of the electrode was 200 nm at Au and 10 nm at Cr. As illustrated in Figure 2.2 B, electrodes with a gap of 15 mm and electrode width of 1mm or 2.5mm were designed and employed to align electrospun fibers over longer distances.

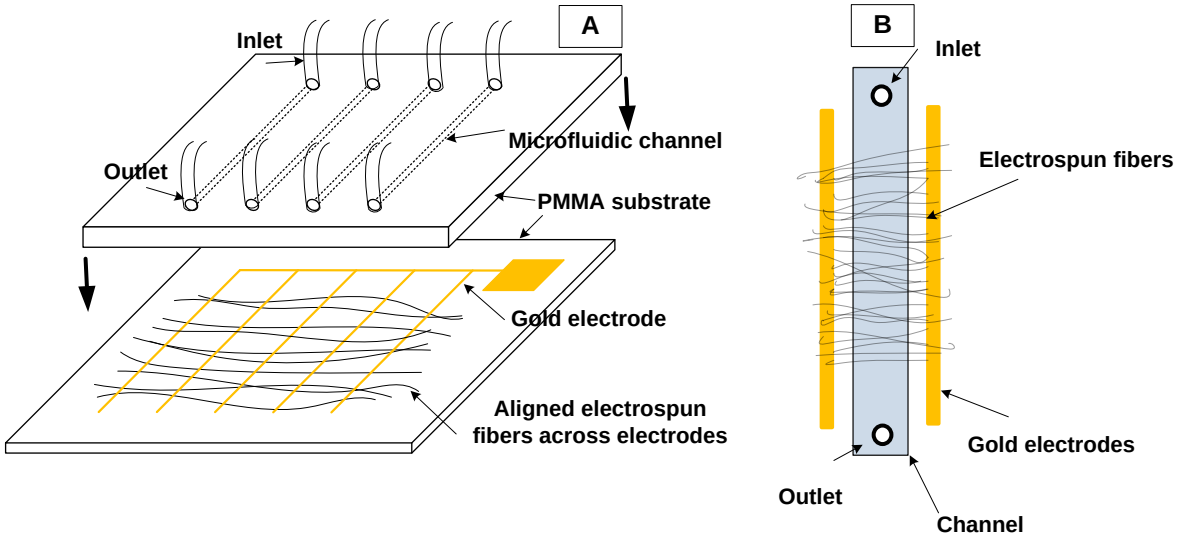

Figure 2.3 Schematic of a microfluidic device showing the formation of a microfluidic channel with fibers aligned across the channel (A) and a top view of a channel incorporated with fibers (B).

Microfluidic PMMA channels were formed by a hot embossing process using a copper template as previously described [112]. Briefly, the channel design on the copper template was

formed by patterning with an epoxy-based resist (KMPR 1050, Micro-Chem Corp., Newton, MA) and copper electroplating. The channels (length 12.5 mm, width 0.66 mm, and depth 37 μm) were embossed in PMMA at 130°C and 5000 lbs in a hot press (Carver, Wabash, IN) for 10 minutes, and 0.78 mm holes were drilled so that inlet and outlet tubing could be inserted. The channels were then sealed with UV-assisted thermal bonding [113]. The PMMA embossed channels were UV treated for 10 minutes using a UVO-Cleaner Model 144AX (Jelight, Irvine, CA) and brought into contact with a PMMA surface containing patterned nanofibers. The surfaces were then bonded by pressing for 10 minutes at 85°C and 5000 lbs in order to form channels containing nanofibers (see Figure 2.3). Finally, tubing was glued into the channel inlets and outlets to allow access for a syringe pump.

2.5. Characterization of nanofibrous membrane

2.5.1. Scanning electron microscopy (SEM)

The morphology of all electrospun fibrous webs was evaluated with a Leica 440 scanning electron microscope (SEM) after the fiber webs were coated with Au-Pd. Image analysis software (ImageJ 1.41) was used to measure the electrospun fiber diameter.

2.5.2 Testing nanofibers in microfluidic channels

Plain DI water was injected through a channel using a syringe pump at 5 and 20 μL/min for 5 min. The effluent was collected to analyze whether the incorporated electrospun fibers were dissolved or not during fluid flow. To make the simulated solutions, the electrospun fibers were dissolved in DI water at 1.0, 0.1, and 0.01 wt% PVA over water. A vial containing DI water and electrospun nanofibers was left in an oven of 65^{o}C for 6 hours for the preparation of three simulated solutions so that FTIR and NMR could be used to compare the effluent.

2.5.3. FTIR and NMR measurement

The electrospun fibers were characterized using FTIR and found to be 800 to 3800 cm^{-1} with a 4 cm^{-1} resolution. To analyze the effluent and the simulated solutions, ^{1}H spectra were recorded with an Inova 400 NMR instrument operating at 400 MHz at room temperature, and FTIR was used to measure the effluent and the simulated solutions.

2.5.4. XPS measurement

XPS experiments were carried out using a model SSX-100 ESCA system with Al Kα radiation (1486.6 eV). XPS analyzes photoelectrons that escape only from the top few mono-layers of a surface making it a very surface-sensitive technique and appropriate for detecting functional groups on the surface of fibers. The operating pressure of the analyzer chamber was about 2×10^{-9} torr. The X-ray spot size was 1 mm x 2 mm and photoemission electrons were collected with an emission angle of 55 degrees. Typical analysis depths were ~5 nm and survey spectra were collected into a hemispherical analyzer using a pass energy of 150 V. The binding energy (BE) values were calculated relative to the C (1s) photoelectron peak at 285.0 eV. Three different locations on each sample were measured to ensure reproducibility.

2.5.5. Thermally stimulated current (TSC) measurement

TSC experiments were carried out to measure the currents generated on the charged nanofibers using a Novocontrol TSC (Novocontrol Technologies, Hundsangen, Germany). TSC spectra were recorded with two blocking electrodes that are specially designed to contain an aqueous solution or a wet nanofiber sample. The cylindrical container with the blocking electrodes is 1 mm in depth and 19 mm in diameter. For the control, no fiber, experiment

container was filled with a pH 7 buffer solution. A pH 7 buffer solution was prepared by adjusting the ratio of monobasic sodium phosphate and dibasic sodium phosphate, which were purchased from Sigma-Aldrich. The mole concentration of the buffer solutions was set as 10 mM. In the absence of an externally applied field, the currents of the buffer solution were measured at 25 ^{o}C for 15 min. In case of the charged nanofibers, 6 mg of the nanofibers was soaked in the buffer solution for 30 min to allow ionization or protonation of functional groups prior to measurement. The wet nanofibers were put in the container and measured in the same way as the buffer solution.

3. Results and Discussion

3.1 Incorporation of functional polymers in PVA nanofibers

All of the prepared spinning dopes were effectively electrospun on aluminum foil, and as shown in Figure 2.4, the electrospun nanofibers showed good morphology without beads on their fiber surface. Although the prepared solutions were subjected to some variation in spinnability, the diameters and morphologies of the electrospun fibers were very similar; the diameters of the pure PVA fibers ranged from 350 nm to 450 nm, the PVA/PB hybrid nanofibers from 450 nm to 550 nm, and the PVA/Poly(MA) hybrid nanofibers from 300 nm to 400 nm. Fiber diameters were sensitive to electrospinning conditions and could be altered slightly by such changes in the electrospinning voltage and the distance between the needle and collector.

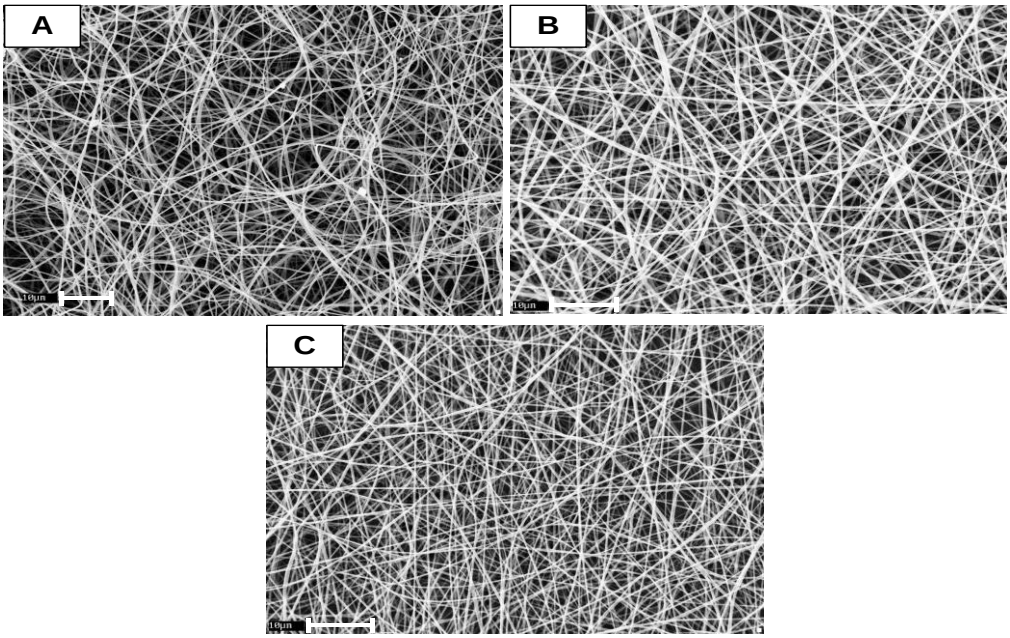

Figure 2.4 SEM images of electrospun fibers on aluminum foil: (A) pure PVA nanofibers, (B) PVA/PB hybrid nanofibers, and (C) PVA/Poly(MA) hybrid nanofibers.

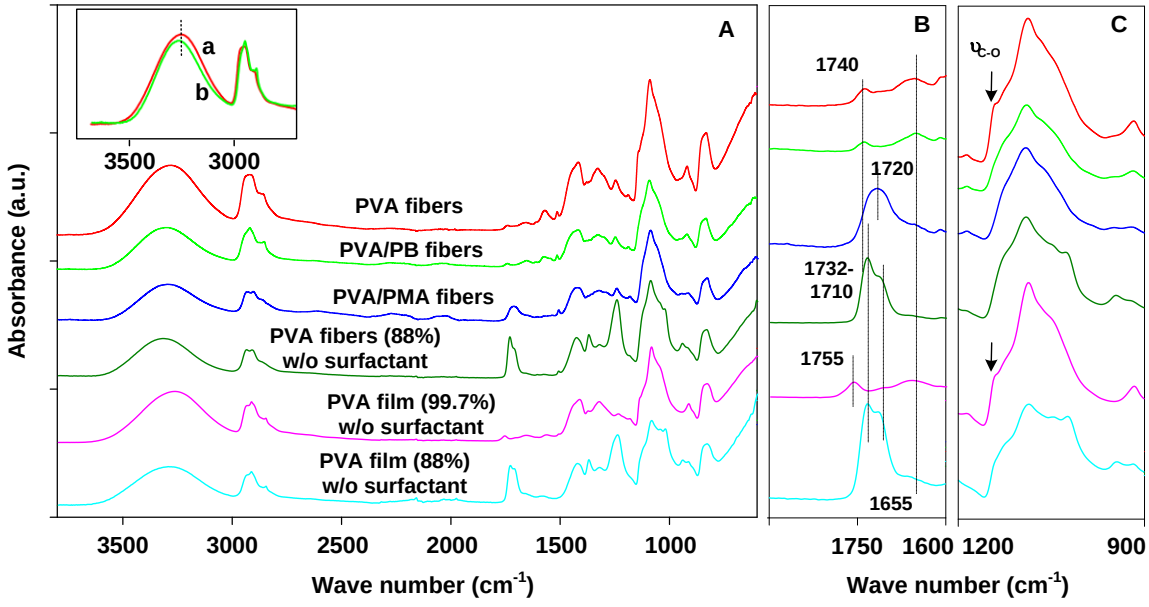

Figure 2.5 FTIR spectra: overall results (A); pure PVA fibers, PVA/PB and PVA/Poly(MA) hybrid nanofibers, PVA fibers made of 88% hydrolyzed PVA polymers without surfactant, and

PVA films made with 99.7% and 88% hydrolyzed PVA polymers (w/o = without), (B) magnified FTIR spectra (1900~1600 cm^{-1}) and (C) (1200~900 cm^{-1}).

3.2 Examination of functional groups within fibers

FTIR and XPS were used to examine the incorporation of PB and Poly(MA) with the PVA polymer. FTIR spectra of four as-spun fiber samples and two film samples are presented in Figure 2.5. The pure PVA fibers, PVA/PB and PVA/Poly(MA) hybrid fibers were prepared with the 99.7% hydrolyzed PVA polymer and the surfactant, Triton X-100. For reference and clarification of the spectra, another PVA fiber sample was spun with a spinning dope made of 88% hydrolyzed PVA polymer without using Triton X-100, and film samples were prepared from PVA polymers with both 99.7% and 88% degrees of hydrolysis. Fibers could not be spun directly from the 99.7% hydrolyzed PVA without using Triton X-100 because of poor spin-ability.

All carbonyl compounds absorb in the region 1760-1650 cm^{-1} due to the stretching vibration of the C=O bond. It notes that C=O stretch of saturated esters (1755-1735 cm^{-1}) is at a higher wavelength than that of the unsaturated esters (1730-1715 cm^{-1}) and that of unsaturated aldehydes and ketones (1710-1650 cm^{-1}). The PVA film (99.7%) shows a very small peak at the 1758 cm^{-1} that is considered a saturated ester compound derived from the non-hydrolyzed poly(vinyl acetate) group, whereas the ester compound observed at 1758 cm^{-1} from the acetate group is shifted to 1740 cm^{-1} in PVA fibers and PVA/PB hybrid fibers during the formation of fibers. Based on the spectra of the PVA fiber (88%) and the PVA film (88%), the acetate group is clearly observed in the broad region of 1732-1710 cm^{-1} as an unsaturated ester compound. Addition of Poly (MA) to the PVA polymers is clearly confirmed by the absorbance peak at 1720 cm^{-1} attributed to the carboxylic group from Poly (MA). A light presence of the peaks at

1655 cm^{-1} is shown in the samples with the striking peaks associated with carbonyl compounds, whereas in the PVA fibers, the PVA/PB fibers, and the PVA film (99.7%) which have the small peaks at 1655 cm^{-1} wavelength, clearer peaks are shown to be considered as an unsaturated aldehyde or ketone compounds. As a result, the carboxyl compounds are variously observed at the different wavelengths according to their formations.

On the other hand, PB has weaker absorbance in the IR region and was difficult to identify with FTIR. FTIR measurements show absorbance peaks to be slightly different among the samples in the peak intensity for O-H at 3550~3100 cm^{-1} and in the peak shape between 1200 ~ 900 cm^{-1}. In the inset of Figure 2.5, the spectra of PVA and PVA/PB fibers were normalized using the peak at 1097 cm^{-1} (C-O stretching vibrations at the non-hydrolyzed group in PVA) [114]. Changes in intensities and shifts in peaks in this region (O-H) reflect hydrogen bonding between PVA and the additive polymers [115]. The O-H peak decreased slightly in intensity and varied in shape with the addition of functional polymers in the PVA fibers. PVA typically forms small, dense, and closely packed monoclinic crystallites [116] and the degree of crystallinity of PVA fibers strongly affects the FTIR C-O stretching peak at 1141 cm^{-1}. As the PVA polymer chains are aligned and folded to make the crystalline structure, the PVA hydroxyl groups form intramolecular and intermolecular hydrogen bonds between PVA chains [117]. In the case of less hydrolyzed-PVA polymers (88%), the film and fiber samples show much weaker shoulder than their counter parts of the 99.7% hydrolyzed PVA polymers. In the meanwhile, incorporation of functional polymers into the PVA fibers resulted in strong association of the PVA hydroxyls so that PVA crystallization was disrupted during electrospinning. As the functional polymers were added, the decrease in 1141 cm^{-1} is clearly observed in the FTIR spectra and no discernible shoulder at 1141cm^{-1} is detected at the hybrid fibers (Figure 2.5 C).

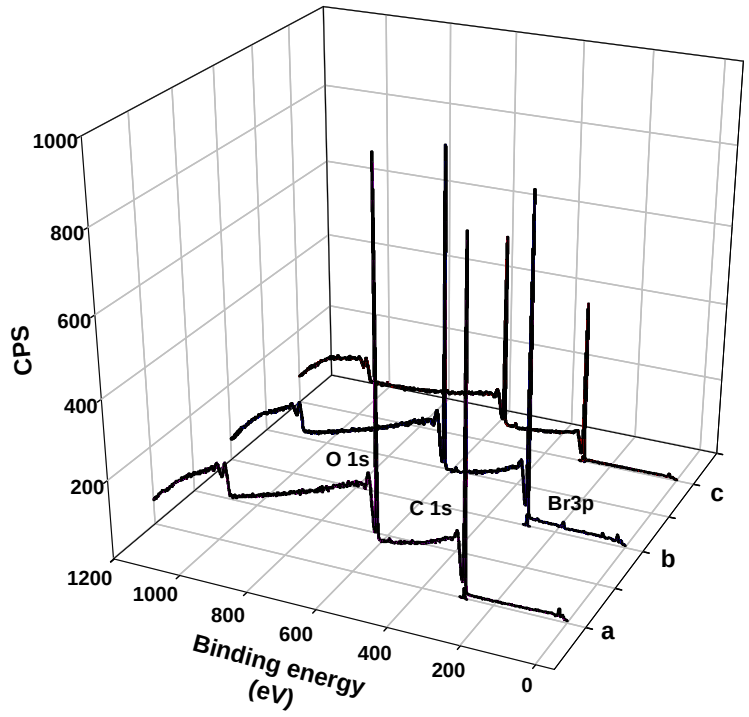

Figure 2.6 XPS spectra of pure PVA electrospun nanofibers (a), PVA/PB hybrid nanofibers (b), and PVA/POLY(MA) hybrid nanofibers (c).

To further investigate the location of the incorporated functional polymers and in particular to have stronger confirmation of PB incorporation, XPS spectra in broad survey mode were recorded to detect and quantify the major atomic elements and bonding patterns at the surface (~ 5 nm depth) of the electrospun fiber samples. XPS peaks correspond to specific energy states of electrons in the s or p orbital of their respective atoms. For PVA/PB fibers, the unique Br nucleus associated with PB was used to quantify the proportion of PB at the fiber surface. In PVA/Poly(MA) nanofibers, no unique nucleus was available and variations in C to O abundance were used to quantify Poly(MA) relative to PVA. XPS survey spectra (Figure 2.6) show the major photoelectron peaks corresponding to the O (1s) and C (1s) at a binding energy of 531 and

285 eV with signal intensities corresponding to the atomic percentage of each element [84]. To evaluate the presence of Br-N associated with PB in the sample surface, the spectra were analyzed in the region of 400 eV and 260 eV ~ 65 eV where signals of nitrogen and bromine, respectively, appear. Although the PB has two nitrogen atoms and two bromine atoms, XPS spectra contained no measurable signal for nitrogen but measurable peaks for bromine on the surface of the PVA/PB hybrid nanofibers. The heavy bromine produces a strong XPS signal because it has high relative sensitivity factor (RSF) of 5.03 in XPS compared to nitrogen (RSF 1.8). The bromine peak area can be 5.03/1.8 compared to the nitrogen peak area for equal amount of bromine to nitrogen. The Br (3p) spectrum was not observed in the pure PVA nanofibers and PVA/Poly(MA) hybrid nanofibers but it was present in the PVA/PB hybrid nanofibers. The amount of bromine in the shell from the fiber surface was determined by comparing the Br/C weight ratio from the results of bromine At % and carbon At % measured by XPS. To calculate the atomic percent (At %) of each element, the weight percent (Wt %) of each element calculated from formulation is divided by its atomic weight and then each result is divided by the total summation of each dividing result.

Table 2.1 Abundance (At %) of elements; measured at the fiber surface by XPS and calculated from formulation

	PVA fibers		PVA/PB fibers		PVA/PMA fibers	
	XPS	Calculated	XPS	Calculated	XPS	Calculated
C	73.7	67.6	74.4	68.6	71.4	67.3
O	26.3	32.4	25.3	30.8	28.6	32.7
Br	-	-	0.4	0.7	-	-

In Table 2.1, the abundance of elements at the fiber surface is presented, in which the At % of each element is listed from both of the data measured by XPS and the results calculated from each fiber formulation. For these calculations, the full composition of the fibers; PVA/triton

X-100: 89/11, PVA/PB/triton X-100: 82/8/10, PVA/POLY(MA)/triton X-100: 82/8/10, was used including the surfactant. With boiling point > 200^{o}C and vapor pressure < 1mm Hg at 20^{o}C little of the Triton X-100 is expected to evaporate during the electrospinning process. In all cases, the surface composition of the fibers, as measured by XPS, was richer in carbon, than the overall fiber formulation (calculated). The XPS measurements have confirmed, perhaps not surprisingly, that the carbon rich Triton- X (molecular formula: $C_{14}H_{22}O(C_2H_4O)_n$ (n = 9-10)) has migrated to the surface of the nanofibers.

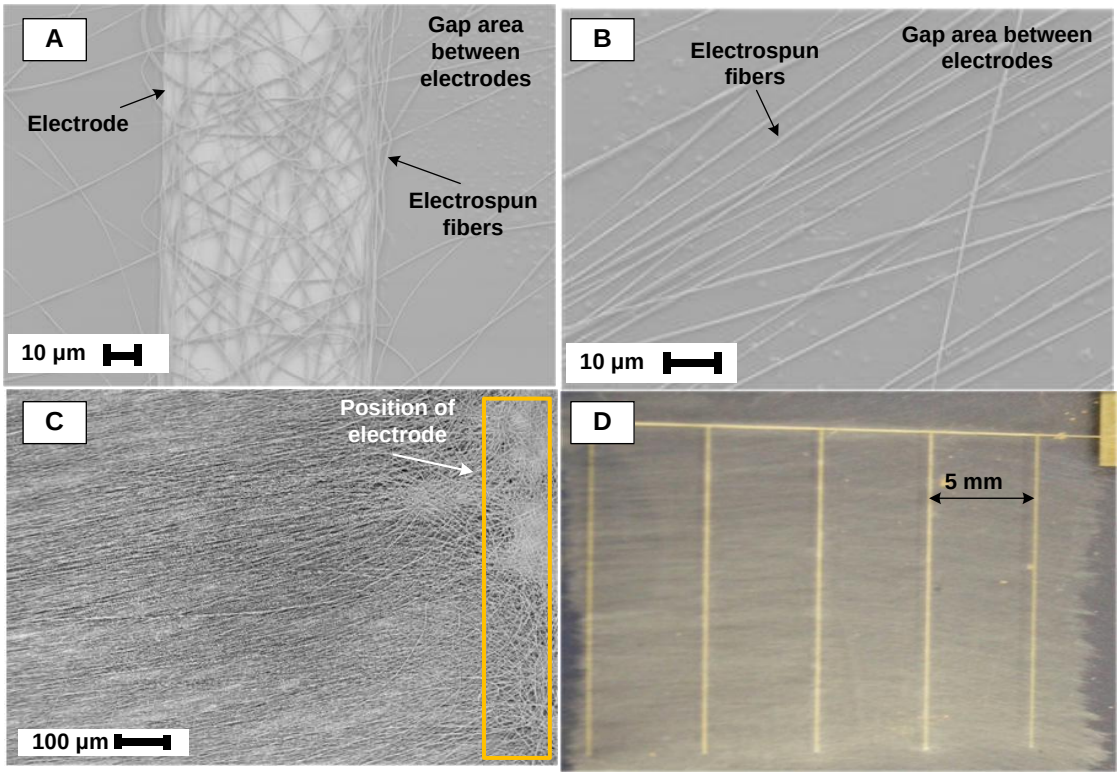

Figure 2.7 SEM (A~C) and photographed (D) images of electrospun nanofibers on the gold electrodes; accumulated nanofibers on an electrode (A) and aligned electrospun fibers across the electrodes (B~D).

3.3 Patterned nanofibers on chips

When fibers were collected on chips with grounded gold electrodes, the expected pattern of random fiber orientation on electrodes and extended, aligned fibers between electrodes was observed. As shown in Figure 2.7 and 2.8, the nanofibers were well aligned between electrodes with gap widths ranging from 0.5 mm to 15 mm, or accumulated on the grounded electrodes. At the shortest gap distances (0.5 mm, Figure 2.7 A), the electrospun nanofibers were stacked on the electrodes and the alignment of nanofibers across the short gap was poor. Increasing the distance between electrodes improved the overall alignment of fibers between electrodes. As the width between the electrodes was increased to 15 mm, the width of the electrode was also found to be important. Fibers electrospun onto chips with thin electrodes (1 mm gold width) spaced 15 mm apart were not well aligned. When the gold electrode width was increased to 2.5 mm, however, the electrospun fibers were well aligned over the 15 mm gap between electrodes (Figure 2.8 B). This phenomenon was attributed to insufficient effectiveness of the grounding on the 1mm electrodes. In our experiment, a 5 mm gap between two neighboring electrodes resulted in excellent nanofiber alignment. Therefore, multiple electrodes with 5 mm gaps were fabricated on a PMMA chip for further processing into microfluidic channels (Figure 2.7 D) with the nanofibers perpendicular to the channel length.

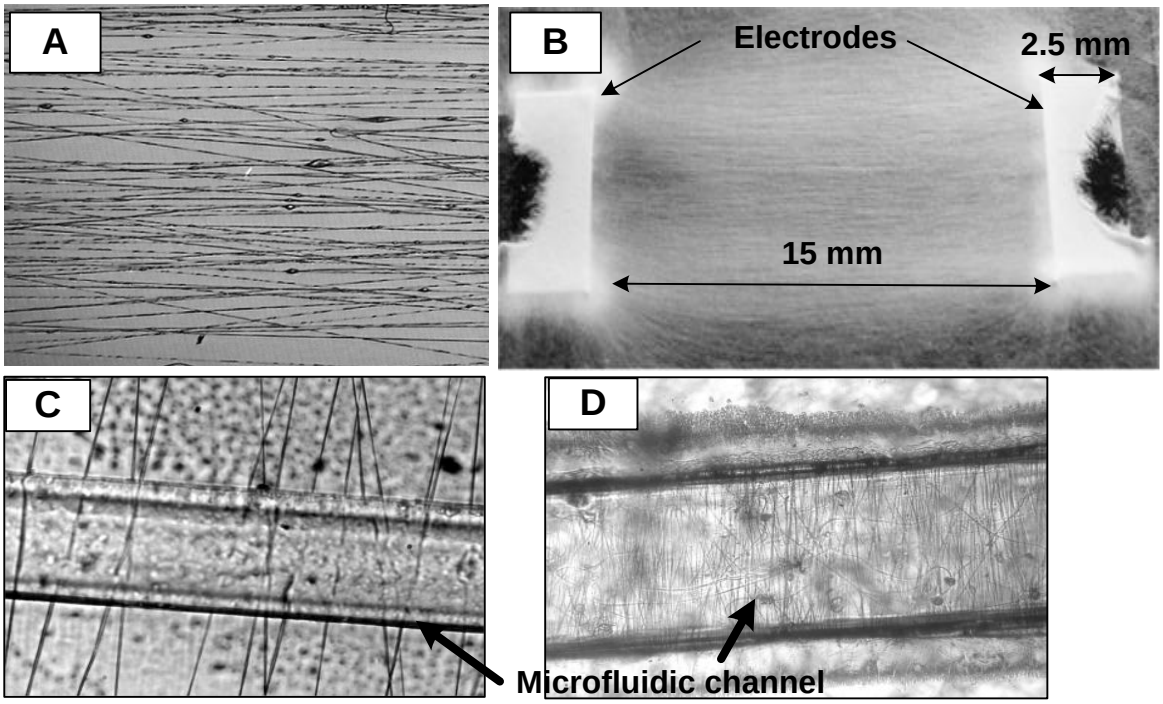

Figure 2.8 Light microscope images of nanofibers aligned along the gold electrodes (a magnification lens of 10x (A) and of 1.5x (B)), nanofibers aligned across channels in assembled microfluidic devices (at low (C) and high fiber density (D)).

3.4 Investigation of incorporated nanofibers in a microfluidic channel

Assembly of the full microfluidic device incorporating electrospun nanofibers across channels (Figure 2.3) required high pressure, temperature and UV exposure to insure that no leakage would occur when fluids flow through the channels. Images of assembled devices (Figure 2.8 C, D) confirm that the electrospun nanofibers maintained alignment and were stable to the chip fabrication process. To determine that these fibers would also be stable during microfluidic device use, nanofibers aligned across the microfluidic channel were tested for their stability during fluid flow through the channels. As a bio-application material, the physical features of the PVA polymer are both strong and weak. The strength is in the hydrophilic property that enhances the interaction of analytes in aqueous solutions. The weakness is the

potential dissolution or breakage of the fibers in flowing, aqueous systems, which is likely to destroy the morphology of the electrospun PVA nanofibers.

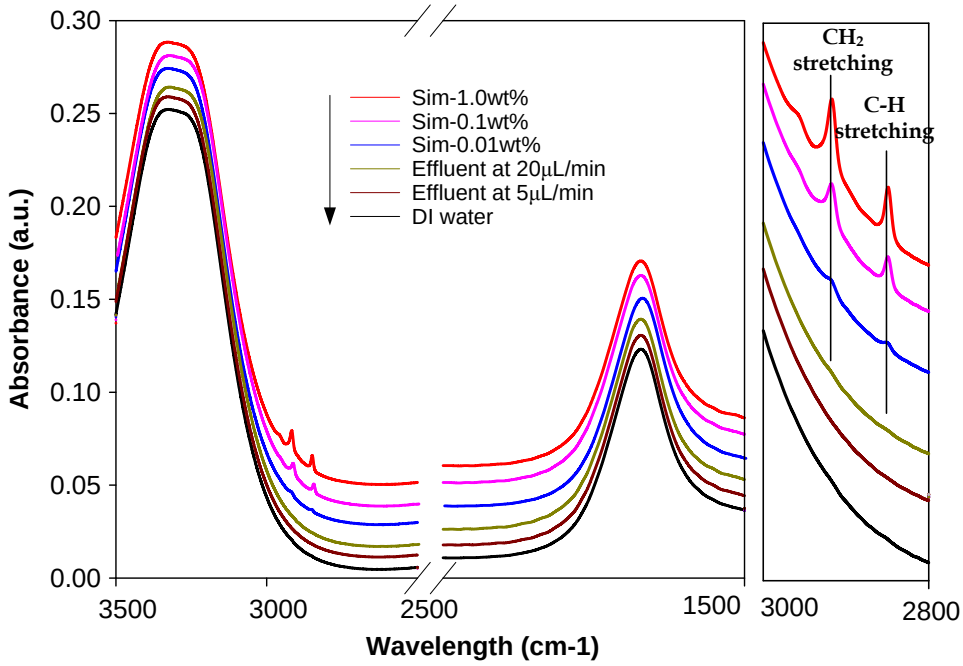

Figure 2.9 FTIR spectra of three simulated solutions, two effluents, and DI water.

The solutions were collected from the outlet of the microfluidic device to test the durability of the electrospun nanofibers in the aqueous solutions. To collect the effluent, DI water was flushed through the channels at high flow rates (for microfluidic devices) of 5 μL/min and 20 μL/min (linear velocities of 3.4 and 13.6 mm/s) for 400 min and 100 min, respectively. The polymer component elements were analyzed in the effluents using FTIR and H-NMR. A set of standard/calibration specimens were also prepared by dissolving electrospun PVA fibers in DI water at 1.0, 0.1, and 0.01 wt%. In FTIR analysis (Figure 2.9), two characteristic peaks for CH_2 at 2930 cm^{-1} and CH at 2850 cm^{-1} were identified. These two peaks originated from PVA nanofibers that had been dissolved and could be identified at PVA concentrations as low as 0.01

wt%. These peaks could not be detected in the effluent collected from the microfluidic channels or in the negative control sample (DI water).

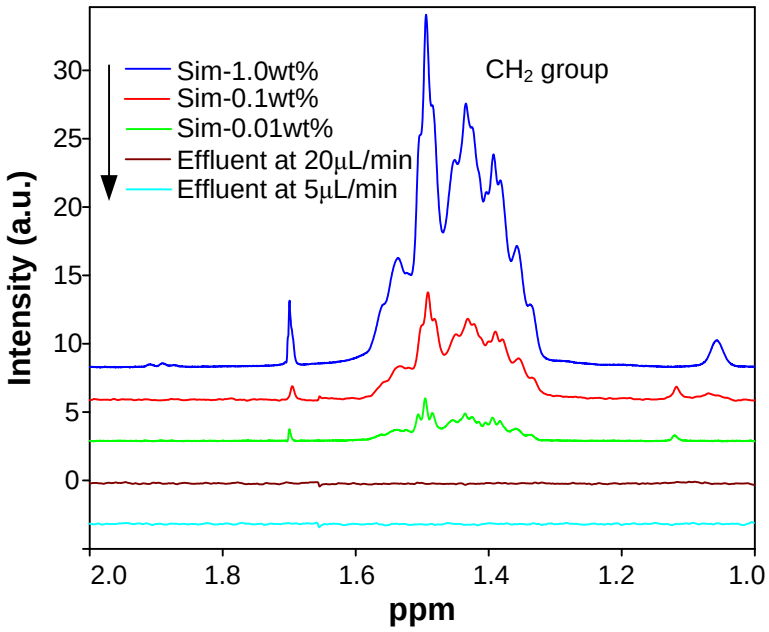

Figure 2.10 H NMR spectra of the calibration solutions and two effluents.

H NMR provided additional evidence that fibers were stable within the microfluidic channels and did not dissolve or wash out even at high flow rates. In the ^{1}H NMR spectra for control samples (Figure 2.10) peaks were present at 1.3~1.6 ppm, characteristic of CH_2 in PVA polymer. These peaks were easily identified at all control sample concentrations. As in the FTIR data, nothing was detected in the effluents from the microfluidic devices. The quantity of dissolved PVA polymers in the solutions was estimated so that the presence or absence of these polymers could be assessed. In conclusion, the electrospun PVA nanofibers incorporated in the microfluidic device maintained stability in fiber morphology during fluid flow. The results of FTIR and ^{1}H NMR demonstrate that PVA electrospun nanofibers are sufficiently stable in the channel to be used in microfluidic devices for bio-analysis.

3.5 Currents of charged nanofibers

TSC measurements demonstrated clear differences between the PVA/PB and PVA/Poly(MA) fibers (Figure 2.11). As a control, current generated in the TSC container by the pH 7 buffer solution was measured and shown to have a small positive charge potential confirming that the buffer has vanishingly small ionic strength. As expected, the PVA/PB nanofibers generated a positive current, whereas the PVA/Poly(MA) nanofibers generated negative current. The total current flowing in circuit is the sum of current carried by electrons and current carried by ions. Therefore, the polarity of the materials governs the direction of total current. From these results, functional groups on the PVA/PB hybrid nanofibers are protonated creating a positive surface potential and a positive current in the solution. On the other hand, ionization of the functional groups on the PVA/Poly(MA) hybrid nanofibers results in a negative surface potential and negative current in the solution. As time lapses, the current intensity for both nanofibers decays slightly. This intensity decrease indicates that the ions in the buffer solution around the nanofibers become saturated on the electrodes and the concentration of ions inducing the currents decreases.

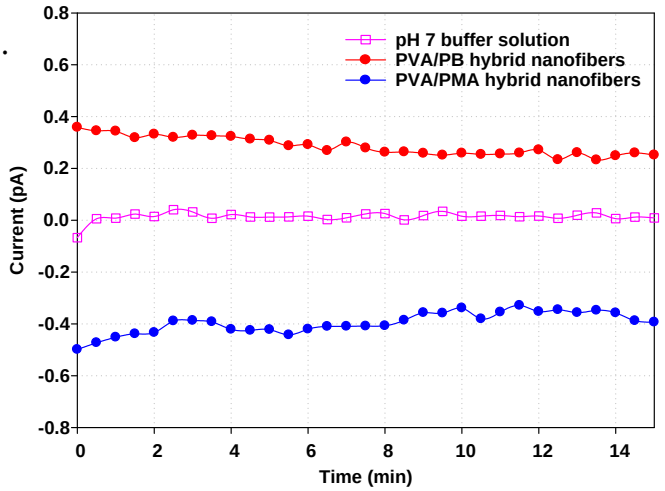

Figure 2.11 TSC spectra showing the relationship between current versus time with a pH 7 buffer solution and the charged nanofibers soaked in the buffer solution.

4. Conclusion

The nanofibers in this study were fabricated in order to create patterns on the PMMA chip with gold electrodes and integrated into polymer-based microfluidic channels to create functionalized microfluidic systems. Functional polymers with charged chemical groups and a surfactant were successfully incorporated into PVA nanofibers and incorporation of the additives and migration of the surfactant to the fiber surface was confirmed by XPS and FTIR testing. The alignment of nanofibers between two electrodes was achieved by grounding the electrodes and charging the spinneret of the electrospinning device. Fibers were successfully aligned at lengths up to 15 mm. Thus, it is possible to influence the layout of the nanofibers within and across microfluidic channels via electrode placement, size and design. This will be further exploited in future research by creating nanofiber tufts within microfluidic channels, using them as guiding lines along a channel. A gap between two electrodes of 5 mm was chosen to prepare aligned electrospun nanofibers for further assembly into microfluidic devices with nanofiber aligned perpendicular to the fluid flow direction within microfluidic channels. An evaluation of the hydrophilic nanofibers showed that the nanofibers maintained morphology during flow of DI water at high rates through the microfluidic channel. Further studies have been carried out using these microfluidic nanofiber systems for sample concentration assays [118] and zeta potential measurements in situ [119].

Acknowledgements

Dr. Daehwan Cho is the first author of this paper. It was included within this thesis to provide necessary background for the third chapter.

The authors are grateful for the financial support from NSF CBET-0852900 and the National Textile Center. Partial funding for this research was also provided by the Cornell Agricultural Experiment Station through federal funding project 356 : " Novel Nanofiber Biosensor for Food Safety"

CHAPTER 3

Functionalized Electrospun Nanofibers as Bioseparators in Microfluidic Systems

Abstract:

In this work, functionalized electrospun poly(vinyl alcohol) (PVA) nanofiber mats were shown to successfully serve as bioseparators for negatively charged nanoparticles. Nanofibers were electrospun onto gold microelectrodes, which were incorporated into poly(methyl methacrylate) (PMMA) microfluidic devices using UV-assisted thermal bonding. PVA nanofibers doped with hexadimethrine bromide (polybrene) were positively charged and successfully filtered negatively charged liposomes out of a buffer solution, while negatively charged nanofibers doped with poly(maleic anhydride) (POLY(MA)) were shown to repel the liposomes. In addition, the effect of fiber mat thickness was studied in order to determine the optimal range of thicknesses for liposome retention. Finally, it was demonstrated that liposomes bound to positively charged nanofibers could be selectively released using a HEPES-sucrose-saline (HSS) solution of pH 8.5 rendering the positively charged nanofibers negatively charged. The results prove that nanofibers can be successfully used for sample preparation procedures of isolation and concentration in lab-on-a-chip devices.

1. Introduction

Micro-total analysis systems (μTAS) incorporate sample preparation and analyte detection into one device that utilizes small feature sizes and volumes in the nano to microliter range. These miniaturized detection assays are portable and permit fast sample analysis and low reagent consumption[1, 79, 120]. These systems can also be designed to allow for parallel

processes, permitting multi- analyte detection within one device. However, the decreased sample volumes and smaller feature sizes of these miniaturized devices result in a lower tolerance for particulates and sample impurities [1]. In addition, significant analyte concentration is necessary in order to reduce sample volumes to the nL-µL ranges used by these devices. While there have been several successful µTAS devices developed, incorporating sample purification and concentrations in the same device as analyte detection remains a key challenge for many analysis systems [79]. This research addresses the need for sample preparation within lab-on-a-chip devices through the incorporation of functionalized electrospun nanofibers within polymer microfluidic devices.

Electrospinning is a fiber formation process that uses electrical forces to generate fibers with diameters on the order of 100 nm [3]. The nonwoven mats formed during electrospinning feature extremely large surface area to volume ratios, and can be tailored to have different pore sizes and tensile strengths [3]. Additionally, electrospun nanofibers can be functionalized with a wide range of surface chemistries through the incorporation of true nanoscale materials in the spinning dope [75, 117, 122]. Several interesting fiber chemistries have been developed that would be ideal for use within microfluidic biosensors. Li *et al.* have successfully electrospun biotinylated nanofibers capable of binding streptavidin in solution [75, 121]. In addition, conductive nanofibers have been created using polyaniline, carbon nanotubes, and other conductive materials [123,124]. Functionalized nanofibers have previously been incorporated within membranes to allow for immuno and optical sensing [5, 125, 126]. In these applications, nanofibers can be functionalized by adsorbing or covalently bonding antibodies to the fiber surfaces, allowing for detection using colloidal gold, latex beads, or liposomes [127]. Finally,

graphite and carbon nanofibers have been used to form micro and nanoelectrodes within electrochemical biosensors [128, 129].

Several groups have examined the feasibility of incorporating electrospun nanofibers within microfluidic systems. It has been demonstrated that nanofibers maintain their morphology when free floating in low Reynolds number flows [98]. Nanofibers have also successfully been used as scaffolds for cell growth within microfluidic devices [130,131]. Recently, we have demonstrated the feasibility of incorporating functionalized PVA nanofibers as filters within microfluidic channels using gold microelectrodes [74]. Positively and negatively charged nanofibers were created by incorporating polybrene and Poly(MA) respectively within a PVA spinning dope. These nanofibers were incorporated within PMMA microchannels using UV-assisted thermal bonding and were shown to maintain their morphology and functionality in fluid flows up to 20 µL/min for 100 minutes.

In this study, we examine the potential of functionalized electrospun nanofibers to address the need for sample preparation within µTAS devices. The controlled capture and release of negatively charged liposomes containing sulforhodamine B were studied using positively and negatively charged PVA nanofibers within microfluidic channels. The effects of fiber mat thickness, charge, and buffer pH were studied in order to determine the ideal conditions for liposome filtration within microfluidic systems.

2. Methods

2.1 Microelectrode fabrication

Gold microelectrodes were patterned onto PMMA to serve as grounded collector plates for nanofiber spinning. Electrodes were composed of 1 mm fingers spaced 5 mm apart connected

to a large square grounding pad (Figure 3.1). The microelectrodes were fabricated at the Cornell NanoScale Science and Technology Facility (CNF) and the Nanobiotechnology Center (NBTC) using a previously described procedure [74]. Briefly, a CHA Mark 50 evaporator was used to first coat the PMMA pieces with a 10 nm chrome adhesion layer and then a 200 nm gold layer at a deposition rate of 1.5 Å/sec. The gold coated PMMA pieces were coated with Shipley 1813 positive photoresist (Shipley, MA) at 3000 rpm for 30 seconds. The photoresist was then exposed for 11 seconds using an ABM contact aligner and developed in MF 321 for 1 minute (Shipley, MA). The substrates were etched in gold etchant type TFA (Transene, MA) for 1 minute and in chrome etchant for 15 seconds (Cyantek, CA). The remaining photoresist was removed using 100 mM NaOH.

Figure 3.1 A five-fingered microelectrode

2.2 Electrospinning

Nanofibers were spun following a previously described procedure [74]. Briefly, positively and negatively charged nanofibers were produced by adding polybrene and POLY(MA) (Sigma Aldrich) into a PVA spinning dope (Polysciences Inc., PA)[19]. The spinning dope was produced by dissolving 10 wt% PVA into deionized (DI) water in an oven at 95 ºC for four hours. To create positively charged nanofibers, polybrene was dissolved in DI water at room temperature and mixed with the PVA solution in a 90/10 wt/wt PVA/polybrene ratio. The resulting solution was vortexed for 2 minutes. Triton X-100 was added to the solution and mixed on a vortex for 2 minutes and an arm-shaker for 1 hour. Negatively charged nanofibers were produced by adding POLY(MA) instead of polybrene to the PVA spinning dope in a 90/10 wt/wt

PVA/Poly(MA) ratio. The Poly(MA) was first dissolved in DI water by heating it at 90ºC for 15 minutes. Fluorescent nanofibers of either charge were produced by using the procedure described above and dissolving the PVA in a DI water and CDot solution. The DI water and CDot solution was produced in a 70/30 wt/wt ratio. CDots were provided by the Wiesner Lab at Cornell University. The CDots contain rhodamine isothiocyanate (TRITC) and produce fluorescent signals when excited at 541 nm (emission at 572 nm).

The spinning solution was loaded into a 5 mL BD plastic syringe with an 18 gauge needle. A positive charge was applied to the syringe needle using a high voltage power supply set at 15 kV (Gamma High Voltage Research Inc., FL). Gold microelectrodes were placed on top of a grounded copper plate and placed 15 cm from the syringe tip. A syringe pump was used to accelerate the spinning solution from the syringe tip at a flow rate of 0.54 mL/h.

2.3 Channel formation and device fabrication

Microfluidic channels were embossed into PMMA using a copper template [112]. Copper templates were fabricated at the CNF using photolithography with KMPR 1050 (Micro-Chem Corp., MA) and copper electroplating to generate raised copper channels on a copper plate. Channels 52 μm deep and 1 mm wide were embossed into PMMA using a Carver Laboratory Hot Press at 130 °C for 5 minutes at 10,000 lbs of pressure. Inlet and outlet

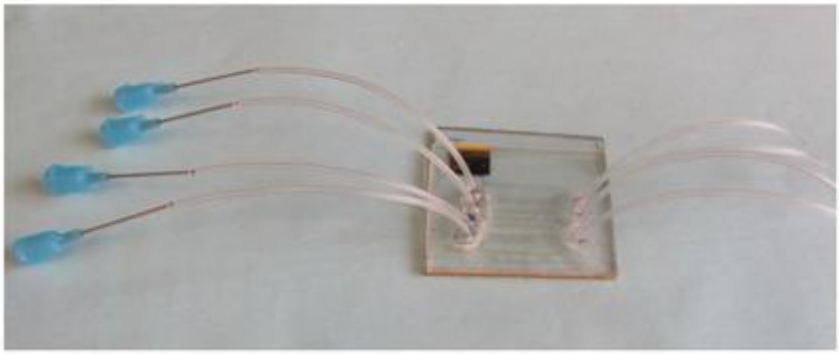

Figure 3.2 Completed microfluidic device consisting of four channels containing functionalized nanofiber mats

holes were drilled at each end of the channel using a 0.8 m steel drill bit. UV-assisted thermal bonding was used to bond the PMMA piece embossed with microchannels and the PMMA piece with the microelectrode and nanofibers. The two PMMA pieces were sandwiched together and pressed on the Carver press for 5 minutes at 90 ºC and 8,000 lbs. Polyvinyl chloride tubing with a 0.02" (0.508 mm) diameter was glued to the inlet and outlet holes (Figure 3.2).

2.4 Liposome retention

Microchannels containing either positively or negatively charged nanofibers were filled with liposomes in a HSS buffer (pH 7) solution (1:1000 v/v dilution to a phospholipid concentration of 11.786 µM) at a flow rate of 1 µL/min. Liposomes were provided by Dr. Katie Edwards in the Baeumner Lab at Cornell University. Liposomes contained 0.44 mol% sulforhodamine B (SRB) conjugated in the lipid bilayer and encapsulated 150 mM SRB to allow for fluorescence imaging (emission 520 nm, excitation 595 nm) [132]. The liposome solution was injected into the channels for 30 minutes and was then washed out using HSS buffer (pH 7) at 1 µL/min for 60 minutes. The concentration of liposomes within the channels was monitored by taking pictures of the channels using a fluorescence microscope. The intensity of fluorescence within the channels was analyzed by using Photoshop to determine the mean red pixel intensity of the images.

2.5 Determining the effect of fiber mat thickness

Fluorescent fiber mats with various thicknesses were spun onto gold electrodes by varying the spinning time. The thickness of the fiber mats was measured using the z-scan function of a Leica SP2 confocal microscope. After imaging, the nanofibers were incorporated into microfluidic devices using the thermal bonding procedure described above. Liposomes in a

1:1000 v/v dilution in HSS (final phospholipid concentration of 11.786 µM) were injected into the channels for 30 minutes and then washed with HSS for 60 minutes to determine the effect of fiber mat thickness on liposome retention. Average red pixel intensity within the channels was assessed using Photoshop.

2.6 Selective liposome release

Microchannels containing positive nanofibers were filled for 30 minutes with a 1:1000 v/v dilution of liposomes suspended in a HSS buffer at a flow rate of 1 µL/min. The channels were first washed for 30 minutes with HSS buffer (pH 7) to ensure that the liposomes had attached themselves to the nanofibers. The channels were then washed with a HSS solution (pH 8.5) in order to determine if it is possible to selectively release the liposomes from the positively charged nanofibers.

3. Results

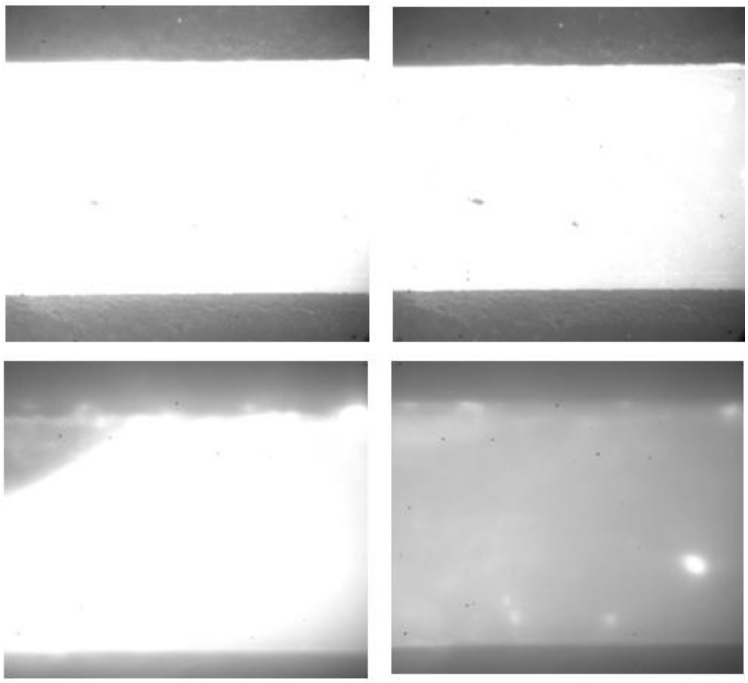

Figure 3.3 (Top) Microchannel containing positive nanofibers full of liposomes (left) and after HSS wash(right). **(Bottom)** Microchannel containing negative nanofibers full of liposomes (left) and after HSS wash (right). Fluorescence microscopy, 100x

3.1 Liposome retention

The ability of functionalized nanofiber mats to filter liposomes out of a buffer solution was assessed using microchannels containing either positively or negatively charged nanofibers. Microfluidic channels containing nanofibers were first filled with a liposome solution (liposomes were diluted in HSS) for

30 minutes and then washed with HSS for 60 minutes. The concentration of liposomes within the microchannels was determined by monitoring the fluorescence in the channels during fluid flow. Channels containing nanofiber mats of either charge gained fluorescence during liposome flow, but only channels containing positive nanofibers retained significant fluorescence after the washing step. Moreover, images of the microchannels during fluid flow demonstrated that the liposomes were bound to the surface of the positive nanofiber mats and remained attached even after an hour of fluid flow (Figure 3.3).

The fluorescence within the microchannels was quantified by using Photoshop to determine the average pixel intensity of the images taken of the channels during fluid flow. Analysis confirmed that the positively charged nanofibers retained significantly more fluorescence than the negative nanofibers (Figure 3.4) with average pixel intensities at steady

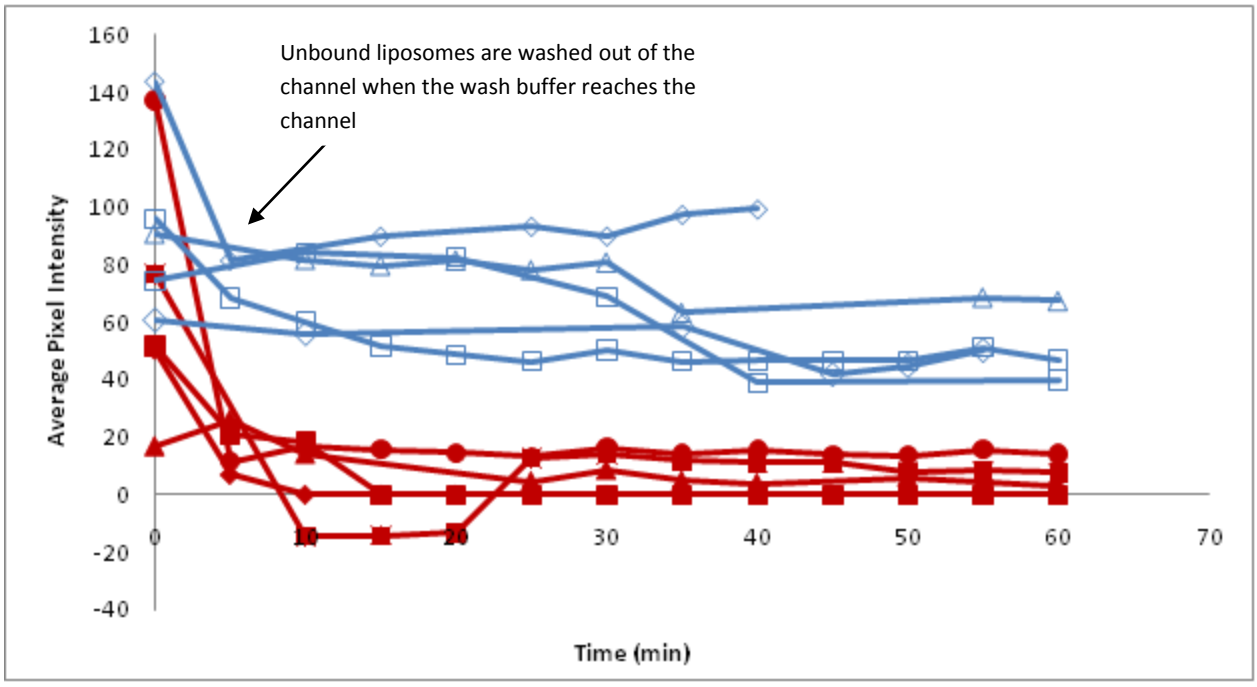

Figure 3.4 A comparison of liposome retention in positively **(blue open symbols)** and negatively **(red solid symbols)** charged nanofiber mats within the microchannels. Liposomes were flown through the device for 30 minutes and then washed out using HSS buffer. Shown here is the step where wash buffer enters the microfluidic channel. The initial high values are due to the pure liposome solution contained within the channels at the beginning of the wash step. Images were taken every 5 minutes and analyzed for red pixel intensity using Photoshop.

state conditions of at least 40 vs. less than 20 respectively. Some variability in the retention of the different fiber mats after HSS was observed, which was attributed to variations in the fiber mat thickness and morphology.

3.2 Effect of fiber mat thickness

The effect of fiber mat thickness on liposome retention was determined by electrospinning nanofiber mats of different thickness between 15 µm and 55 µm. We wanted to determine the minimum nanofiber thickness required for liposome isolation while also determining at what thickness retention becomes a function of pore size and not charge interaction. This was accomplished by comparing the retention behaviors of similarly thick positive and negative nanofiber mats. Each nanofiber mat was imaged using a Leica SP2 confocal microscope to determine fiber mat morphology and thickness (figure 3.5).

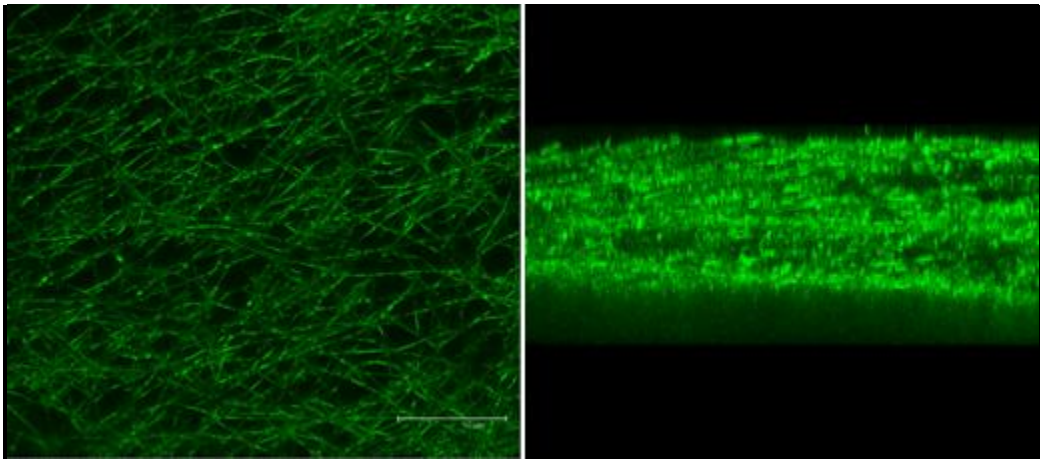

Figure 3.5 Confocal images showing the **(left)** top and **(right)** side of a positive nanofiber mat containing CDots. CDots contain TRITC and enable fluorescence detection (emission 572 nm, excitation 541 nm)

After confocal measurement, the PMMA chips containing the nanofiber mats were bonded to PMMA chips embossed with microchannels as described above. The completed

microfluidic devices were filled with liposomes in HSS buffer for 30 minutes and then washed with HSS buffer for 60 minutes. The liposome retention within the microchannels was analyzed using the average pixel intensity of the channel images during fluid flow. It was determined that negative fiber mats had significant liposome retention at fiber mat thicknesses above 40 μm, indicating that liposomes may be retained because of size exclusion and not charge interaction. Curves similar to those previously shown in Figure 3.4 were obtained. Steady state was reached for all nanofiber mats after 5-20 minutes. The average steady state signals for each fiber mat were determined by averaging the pixel intensity for each mat over 45 minutes (Table 3.1). Positively charged nanofiber mats showed optimal liposome retention at thicknesses of approximately 20 μm and above. The retention of liposomes within the nanofiber mats depends not only on the thickness of the nanofiber mat, but also on its cross-sectional surface area and pore size. Therefore, the nanofiber mat that was 33 μm thick retained more liposomes than the 46 μm nanofiber mat because of its larger cross-sectional surface area and smaller pore size. Some variability in surface area and poor size is to be expected with electrospun nanofibers, however, all the nanofiber mats with thicknesses of 20 μm and above retained a significant number of liposomes.

Fiber Charge	Fiber mat thickness	Average Pixel Intensity
Negative	19 μm	0
	25 μm	-4
	28 μm	2.5
	41 μm	8.1
	47 μm	4.9
Positive	15 μm	1.9
	19 μm	19.6
	29 μm	24.5
	33 μm	55.6
	46 μm	40.7

Table 3.1 Average fluorescent signal observed during 45 minutes of HSS wash step in fiber mats of varying thicknesses.

Confocal images were taken of the channels after fluid flow to determine how the fiber mats were affected by bonding and fluid flow. It was determined that the majority of fiber mat thickness is preserved during bonding and liposome flow (Table 3.2). Additionally, comparing the fluorescence of the nanofibers before fluid flow and after liposome flow and wash gave us more insight into the liposome binding behavior of the nanofiber mats. As expected, the fluorescence observed in the positive fiber mats was dramatically higher after liposome flow and HSS wash (Figure 3.6).

Thickness before bonding	Thickness after fluid flow	Difference
23.5 µm	23.5 µm	0.00 µm
23.5 µm	22.1 µm	1.3 µm
18.2 µm	15.6 µm	2.6 µm
20.2 µm	15.6 µm	4.6µm
44.3 µm	26.1 µm	18.2 µm
44.3 µm	31.3 µm	13.0 µm
44.3 µm	43.6 µm	0.7 µm
39.1 µm	33.9 µm	5.2 µm

Table 3.2 A comparison of nanofiber mat thickness before and after fluid flow

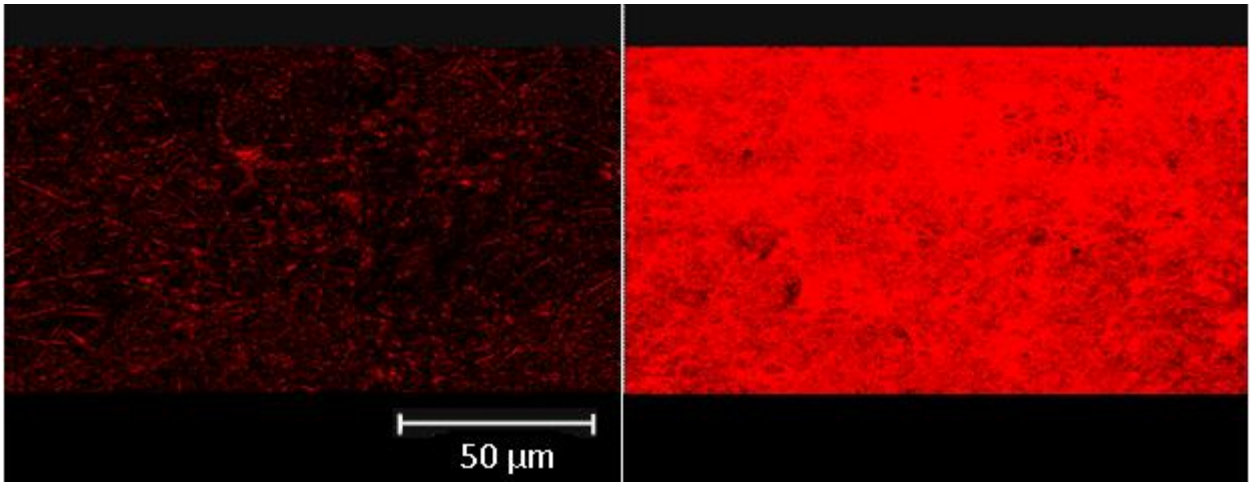

Figure 3.6 A comparison of fiber mat fluorescence **(left)** before and **(right)** after liposome flow and HSS wash

3.3 Selective liposome release

Liposomes provided by Dr. Katie Edwards contained0.44 mol% sulforhodamine B (SRB) conjugated within the lipid bilayer and encapsulated 150 mM SRB to facilitate fluorescence imaging. Their zeta potential is negative over a wide pH range (pH 1-11), while polybrene-modified nanofibers have a negative surface charge at pH 8 and above. Therefore, it should be possible to selectively release liposomes that are bound to polybrene-modified nanofibers using a HSS solution with a pH of 8.5. Channels filled with polybrene nanofibers were filled with liposomes in a HSS buffer (pH 7) and were then washed with HSS buffer (pH 7) to demonstrate that the liposomes were successfully bound to the nanofibers (Figure 3.7). The concentration of liposomes within the solution was determined by imaging channels with a fluorescence microscope. As expected, liposomes were successfully bound by the nanofibers. The signals correlated well with those determined earlier with similarly thick nanofiber mats of 25 µm. After 30 minutes, HSS solution (pH 8.5) was injected into the channels. During the pH 8.5 wash, the channels demonstrated a 50% loss of fluorescence, indicating that liposomes were successfully released from the nanofibers as the remaining fluorescence was general background fluorescence in the system (Figure 3.7).

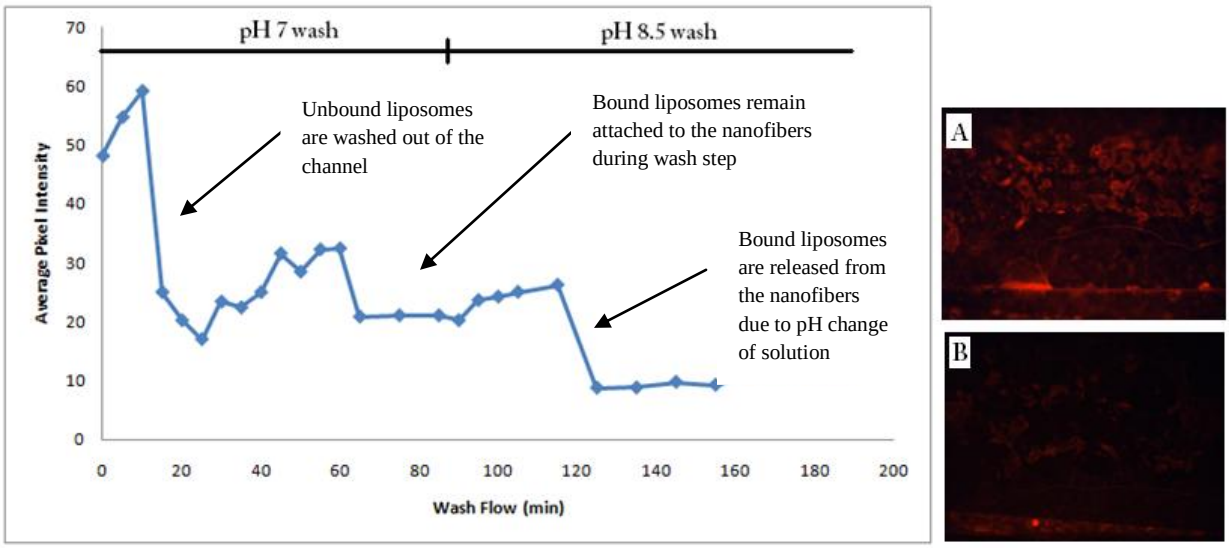

Figure 3.7 Analysis of liposome retention within Polybrene-modified PVA nanofibers during pH7 and pH 8.5 wash. **(A)** Fluorescence image of channel during pH 7 wash **(B)** Fluorescence image of channel during pH 8.5 wash

4. Conclusions

Sample preparation remains a key challenge in the design of µTAS devices, as most analytes are contained in complex matrices that require significant purification and concentration to allow for analyte detection. In this study, we have shown that functionalized PVA nanofibers have the potential to address this challenge through the selective binding and release of particulates or analytes within samples. Functionalized PVA nanofibers were incorporated into PMMA microchannels to allow for filtration of negatively charged liposomes out of a buffer solution. Positively charged Polybrene nanofibers were shown to successfully bind liposomes, while negatively charged Poly(MA) nanofibers were shown to repel the liposomes. Further, we determined that nanofiber mats above 20 µm thick demonstrated optimal liposome filtration. Finally, we demonstrated that bound liposomes can be selectively released from the nanofiber mats using a HSS solution of pH 8.5. Future work will focus on the purification and concentration of analytes from real complex matrices. Here, isolation of diluted analytes from

solution within a small nanofiber mat can be accomplished and combined with detection of the bound or released analytes leading to the development of lab-on-a-chip devices with integrated functionalized nanofibers.

CONCLUSIONS AND FUTURE OUTLOOK

The incorporation of nanoscale materials within biosensors is being investigated as a means of detecting low concentrations of analytes without utilizing amplification processes such as PCR and NASBA. These materials are characterized by extremely large surface areas, resulting in an increased number of binding sites for biological recognition element immobilization. Additionally, nanoscale materials can allow for faster mass transfer rates, ultimately resulting in lower limits of detection and faster analysis than what is seen in traditional sensors. While carbon nanotubes have been successfully used within electrochemical biosensors, their performance is highly dependent on their morphology, which can be difficult to precisely control during synthesis. Consequently, nonwoven nanofiber mats and arrays are being examined as an alternative for sensitive analyte detection.

Nanofiber mats and arrays can provide a much larger functionalized surface area than other nanomaterials, further increasing the number of immobilization sites within a sensor. In addition, nanofibers can be made from a range of biocompatible materials and can be functionalized using other nanoscale materials, such as gold nanoparticles and biological molecules. Finally, most methods of nanofiber synthesis are well understood and can reproducibly produce nanofiber mats or arrays with specific morphologies and mechanical properties.

Currently, many groups are using nanofibers to increase electrode surface area or allow for high density enzyme immobilization within electrochemical biosensors. In general, the increased surface area provided by the nanofibers does result in improved biosensor sensitivity and lower limits of detection when compared to conventional sensors. In addition, utilizing

nanofiber mats has been shown to increase the functional surface area available for detection when compared to other nanomaterials, such as carbon nanotubes. Vertically aligned carbon nanofiber arrays, on the other hand, are encapsulated within polymer matrices and do not show an improvement in terms of available surface area when compared to carbon nanotubes. They do, however, allow for more sensitive detection than that seen in traditional sensors.

While the ability of nanofiber mats to improve electrochemical detection through increasing the surface area of already-existing electrodes has been extensively shown, the use of conductive nanofibers to form electrodes within a microfluidic channel has yet to be demonstrated. The creation of high surface area electrodes out of conductive electrospun nanofibers within microfluidic channels should be investigated. This could result in simpler device fabrication, requiring no complex photolithography steps. In addition, it could allow for the design of easily functionalized electrodes through the inclusion of nanoscale materials within the nanofiber spinning dopes. For instance, gold nanoparticles could be electrospun within the fibers to facilitate electron transfer in the resulting electrodes. In addition, biological molecules, such as enzymes, could also be incorporated within the nanofibers to permit analyte detection.

In this work, we also demonstrate the feasibility of using functionalized electrospun nanofibers for sample preparation within microfluidic biosensing devices. Nanofiber mats spun across a microfluidic channel form a high surface area filter capable of selectively binding particulates or analytes out of a solution. Preliminary studies demonstrated the feasibility of using positively charged nanofibers to filter negatively charged nanovesicles out of a buffer solution. This same simple technology is currently being applied to the concentration and detection of *E. coli* in apple juice.

Using electrospun nanofibers to perform sample preparation within a microfluidic biosensor has the advantage of allowing sample purification and concentration to take place within the same device as analyte detection. This, in turn, allows for the design of complete Lab-on-a-chip devices that can make analyte detection much more accessible to third world countries, rural areas, and point-of-care facilities where the laboratory equipment traditionally needed for sample preparation are not available. While current studies utilize a single nanofiber mat to perform sample preparation within a microfluidic device, the technology could easily be expanded to create microfluidic channels containing multiple nanofiber mats with different functionalities. This would make it possible to perform several sample preparation steps to take place within the channel, allowing us to work with more complex sample matrices. Additionally, utilizing multiple nanofiber mats, or single heterogeneous nanofiber mats, could allow for multiplexed analyte detection. Different configurations of nanofiber mats, such as tufts of nanofibers within a channel, should also be investigated to allow for biorecognition element immobilization.

Nanofiber mats and arrays have been shown to improve biosensor performance through increasing the functional surface area and improving mass transfer rates over those seen in conventional materials. Though nanofibers are currently almost exclusively used within electrochemical biosensors, their wide range of functionalities and easy synthesis make them ideal candidates for use within a wide variety of biosensors. Further work should concentrate on utilizing the many different nanofiber functionalities available to create lab-on-a-chip devices that can perform all sample preparation and analyte concentration without the use of additional laboratory equipment. Additionally, electrospun nanofibers should be investigated as a means of performing sample purification, concentration, and analyte detection within paper-based

microfluidic biosensors. Nanofiber mats with various functionalities could be incorporated as layers within three dimensional paper-based sensors to provide sample purification or concentration as the sample flows through the mats. Their simple and inexpensive fabrication make electrospun nanofibers suitable for use within the paper-based sensors, which aim to provide affordable and easy-to-use diagnostics to areas where laboratory equipment is generally not available. Utilizing electrospun nanofibers for sample preparation in these and other biosensing devices could help increase the accessibility of diagnostic devices and allow for detection using smaller sample volumes than currently used.

REFERENCES

[1] Nugen SR, Baeumner AJ. Analytical and Bioanalytical Chemistry 2008 ;391(2):451-454

[2] Fong H, Reneker DH. Electrospinning and the Formation of Nanofibers. In *Structure Formation in Polymeric Fibers*, Salem, D. R., Ed. Hanser Publishers: Munich, 2001; pp 225-246

[3] Li D, Xia H. Advanced Materials 2004;16:1151-1170

[4] Vamvakaki V, Tsagaraki K, Chaniotakis N. Analytical Chem 2006;78:5538-5542

[5] Luo Y, Nartker S, Miller H, Hochhalter D, Wiederoder M, Wiederoder S, Setterington E, Drzal L.T, Alocikja E. C. Biosensors and Bioelectronics 2010;26:1612-1617

[6] Spain E, Kojima R, Kaner RB, Wallace GG, O'Grady J, Lacey K, Barry T, Keyes TE, Forster RJ. Biosensors and Bioelectronics 2011;26(5):2613-2618

[7] Claussen JC, Franklin AD, Haque AU, Porterfield DM, Fisher TS. ACSNANO 2009;3(1):37-44

[8] Wang, J. Electroanalysis 2004;17(1):7-14

[9] Patolsky F, Zheng G, Lieber CM. Analytical Chem 2006:4261-4269

[10] Feng C, Khulbe KC, Matsuura T. Journal of Applied Polymer Science 2010;115:756-776

[11] Frenot A, Chronaskis I.S. Current Opinion in Colloid and Interface Science 2003;8:64-75

[12] Lee C, Baker SE, Marcus MS, Yang W, Eriksson MA, Hamers RJ. Nano Letters 2004;4(9):1713-1716

[13] Formhals, A. U.S. Pat. 1,975,504 (1935)

[14] Piperno S, Tse B, Bui S, Haupt K, Gheber LA. Langmuir 2011;27(5):1547-1550

[15] Deitzel JM, Kleinmeyer J, Harris D, Beck Tan NC. Polymer 2001;42:261-272

[16] Doshi J, Reneker DH. Journal of Electrostatics 1995;35:151-160

[17] Huang Z-M, Zhang YZ, Kotaki M, Ramakrishna S. Compos Sci Technol 2003;63:2223-53.

[18] Demir MM, Yilgor I, Yilgor E, Erman B. Polymer 2002;43:3303–9.

[19] Chuangchote S, Sirivat A, Supaphol P. Nanotechnology 2007;18(14)

[20] Moradzadegan A, Ranaei-Siadat S, Ebrahim-Habibi A, Barshan-Tashnizi M, Jalili R, Torabi S, Khajeh K. Engineering in Life Sciences 2010;10(1):57-64

[21] Kim WJ, Chang JY. Materials Letters 2011;65:1388-1391

[22] Huang J, Virji S, Weiller BH, Kaner RB. J. Am. Chem. Soc. 2003;125:314-315

[23] Zhang X, Chan-Yu-King R, Jose A, Manohar SK. Synthetic Metals 2004;145:23-29

[24] Zhang X, Goux WJ, Manohar SK. J. Am. Chem. Soc. 2004;126:4502-4503

[25] Zhang X, Manohar SK. J. Am. Chem. Soc. 2004;126:12714-12715

[26] Klein KL, Melechko AV, Rack PD, Fowlkes JD, Meyer HM, Simpson ML. Carbon 2005;43:1857-1863

[27] Toebes ML, Bitter JH, van Dillen, J, deJong KP. Catalysis Today 2002;76(1):33-42

[28] Aoki K, Ishida M, Tokuda K. J. Electroanal. Chem. 1988;251:63-71.

[29] Jacobs CB, Peairs MJ, Venton BJ. Anal. Chimica Acta. 2010;662:105-127

[30] Arumugam, PU, Chen H, Siddiqui S, Weinrich JAP, Jejelowo A, Li J, Meyyappan M. Biosensors and Bioelectronics 2009;24:2818-2824

[31] Zhang J, Lei J, Liu Y, Zhao J, Ju H. Biosensors and Bioelectronics 2009;24:1858-1863

[32] Hrapovic S, Liu Y, Male KB, Luong JHT. Anal. Chem. 2004;76:1083-1088

[33] Wu L, McIntosh M, Zhang X, Ju H. Talanta 2007;74:387-392

[34] Lee C, Baker SE, Marcus MS, Yang W, Eriksson MA, Hammers RJ. Nano Letters 2004;4(9):1713-1716

[35] McKnight TE, Peeraphatdit C, Jones SW, Fowlkes JD, Fletcher BL, Klein KL, Melechko AV, Doktycz MJ, Simpson ML. Chem. Mater. 2006;18:3202-3211

[36] Koehne J, Chen H, Li J, Cassell AM, Ng HT, Stevens R, Han J, Meyyappan M. Nanotechnology 2003;14:1239-1245

[37] Baker SE, Tse KY, Hindin E, Nichols BM, Clare TL, Hamers RJ. Chem. Mater. 2005;17:4971-4978

[38] Baker, SE, Colavita PE, Tse KY, Hamers RJ. Chem. Mater. 2006;18:4415-4422

[39] Baker SE, Tse KY, Lee CS, Hamers R.J. Diamond Relat. Mater. 2006;15:433-439

[40] Arumugam PU, Yu E, Riviere,R, Meyyappan M. Chemical Physics Letters 2010;499(4-6):241-246

[41] Durst R, Baeumner A, Murray R, Buck R, Andrieux C. Biosensors and Bioelectronics. 1997;12(12):iii

[42] Wu L, Yan G, Ju H. Journal of Immunological Methods 2007;322:12-19

[43] Wu L, Zhang X, Ju H. Anal. Chem. 2007:453-458

[44] Wu L, Zhang X, Ju H. Biosensors and Bioelectronics 2007;23:479-484

[45] Lu J, Drzakm LT, Worden RM, Lee I. Chem. Mater. 2007;19:6240-6246

[46] Yu J, Liu S, Ju H. Biosensors and Bioelectronics. 2003;19:401-409

[47] Zhang J, Lei J, Liu Y, Zhao J, Ju H. Biosensors and Bioelectronics. 2009;24:1858-1863

[48] Tan Y, Kan J, Li S. Sensors and Actuators B. 2011;152(2):285-291

[49] Shkotova LV, Soldatkin AP, Gonchar MV, Schuhmann W, Dzyadevych SV. Materials Science and Engineering:C. 2006;26(2-3):411-414

[50] Dai Z, Yan F, Chen J, Ju H. Anal. Chem. 2003;75:5429-5434

[51] Kausaite-Minkstimiene A, Mazeiko V, Ramanaviciene A, Ramanavicius A. Biosensors and Bioelectronics. 2010;26(2):790-797

[52] Berti F, Todros S, Lakshmi D, Mitcombe MJ, Chianella I, Ferroni M, Piletsky SA, Turner APF, Marrazza G. Biosensors and Bioelectronics. 2010;26:497-503

[53] Dhand C, Sumana G, Datta M, Malhotra BD. Thin Solid Films. 2010;519:1145-1150

[54] Du Z, Li C, Li L, Zhang M, Xu S, Wang T. Materials Science and Engineering:C 2009;29(6):1794-1797

[55] Wang X, Yang T, Jiao K. Biosensors and Bioelectronics 2011;26(6):2953-2959

[563] Chen X, Chen Z, Zhu J, Xu C, Yan W, Yao C. Bioelectrochemistry 2011 Doi: 10.1016/j.bioelechem.2011.05.004

[57] Yang T, Feng Y, Zhang W, Ma S, Jiao K. Journal of Electroanalytical Chemistry 2011;656(1/2):140-146

[58] Yue J, Epstein AJ. J. Am. Chem. Soc 1990;112:2800-2801

[59] Mathebe NGR, Morrin A, Iwuoha EI. Talanta. 2004;64:115-120

[60] Wang XL, Tang T, Feng YY, Jiao K, Li GC. Electroanalysis. 2009;21(7):819-825

[61] Yang J, Yang T, Feng YY, Jiao K. Anal. Biochem. 2007;365: 24–30.

[62] Gomathi P, Ragupathy D, Choi JH, Yeum JH, Lee SC, Kim JC, Lee SH, Ghim HD. Sensors and Actuators B 2011;153:44-49

[63] Jayakumar R, Prabaharan M, Nair SV, Tamura H. Biotechnology Advances 2010;28(1):142-150

[64] de Lima F, Lucca BG, Barbosa AMJ, Ferreira VS, Moccelini SK, Franzoi AC, Vieira IC. Enzyme and Microbioal Technology. 2010;47:153-158

[65] Zhou K, Ahu Y, Yang X, Luo J, Li C, Luan S. Electrochimica Acta. 2010;55:3055-3060

[66] Luo L, Li Q, Xu Y, Ding Y, Wang X, Deng D, Xu Y. Sensors and Actuators B. 2010;145:293-298

[67] Chen H, Yan R, Chai Y, Wang J, Li W. Biotechnol Lett. 2010;32:1401-1404

[68] Malhotra BD, Kaushik A. Thin Solid Films. 2009;518:614-620

[69] Huan X, Ge D, Xu Z. European Polymer Journal 2007;43:3710-3718

[70] Jia, Y, Gong J, Gu X, Kim H, Dong J, Shen X. Carbohydrate Polymers 2007;67:403-409

[71] Doretti L, Ferrara D, Lora S, Schiavon F, Veronese FM. Enzyme and Microbial Technology. 2000;27(3-5):279-285

[72] Tsai Y, Huang J, Chiu C. Biosensors and Bioelectronics. 2007; 22(12):3051-3056

[73] Ren G, Xu X, Liu Q, Cheng J, Yuan X, Wu L, Wan Y. Reactive and Functional polymers 2006;66(12): 1559-1564

[74] Cho D, Matlock-Colangelo L, Xiang C, Asiello P, Baeumner A.J, Frey M.W. Polymer 2011

[75] Li D, Frey MW, Baeumner A.J. Journal of Membrane Science 2006;279:354-363

[76] Baeumner AJ, Pretz J, Fang S. Anal. Chem 2004;76:888-894

[77] Ghanbari KH, Bathaie SZ, Mousavi MF. Biosensors and Bioelectronics 2008;23:1825-1831

[78] Elahi MY, Bathaie SZ, Kazemi SH, Mousavi MF. Analytical Biochemistry 2011;411(2):176-184

[79] Batt CA. Science 2007;316:1579-80.

[80] Goral VN, Zaytseva NV, Baeumner AJ. Lab Chip 2006;6:414-21.

[81] Hudson JA, Lake RJ, Savill MG, Scholes P, McCormick RE. J Appl Microbiol 2001;90:614-21.

[82] Veleirinho B, Lopes-da-Silva JA. Process Biochem 2009;44:353-6.

[83] Xiang CH, Frey MW, Taylor AG, Rebovich ME. J Appl Polym Sci 2007;106:2363-70.

[84] Li D, Frey MW, Vynias D, Baeumner AJ. Polymer 2007;48:6340-7.

[85] Kotek R. Polym Rev 2008;48:221-9.

[86] Nisbet DR, Forsythe JS, Shen W, Finkelstein DI, Horne MK. J Biomater Appl 2009;24:7-29.

[87] Botes M, Cloete TE. Critical Reviews in Microbiology 2010;36(1):68-81.

[88] Kriegel C, Arrechi A, Kit K, McClements DJ, Weiss J. Crit Rev Food Sci Nutr 2008;48:775-97.

[89] Schiffman JD, Schauer CL. Polym Rev 2008;48:317-52.

[90] Agarwal S, Wendorff JH, Greiner A. Adv Mater 2009;21:3343-51.

[91] Dalton PD, Joergensen NT, Groll J, Moeller M. Biomed Mater 2008;3:034109/034101-/11.

[92] Freed LE, Engelmayr GC, Jr., Borenstein JT, Moutos FT, Guilak F. Adv Mater 2009;21:3410-8.

[93] Ye P, Xu Z-K, Wu J, Innocent C, Seta P. Biomaterials 2006;27:4169-76.

[94] Wang G, Ji Y, Huang X, Yang X, Gouma P-I, Dudley M. J Phys Chem B 2006;110:23777-82.

[95] Wang X, Drew C, Lee S-H, Senecal KJ, Kumar J, Samuelson LA. Nano Lett 2002;2:1273-.

[96] Reneker DH, Yarin AL. Polymer 2008;49:2387-425.

[97] Yang H, Dong L. Langmuir 2010;26:1539-43.

[98] Sadlej K, Wajnryb E, Ekiel-Jezewska ML, Lamparska D, Kowalewski TA. Int J Heat Fluid Flow 2010;31:996-004.

[99] Lee KH, Kwon GH, Shin SJ, Baek J-Y, Han DK, Park Y, Lee SH. J Biomed Mater Res Part A 2009;90A:619-28.

[100] Lee KH, Kim DJ, Min BG, Lee SH. Biomed Microdevices 2007;9:435-42.

[101] Ma Z, Kotaki M, Yong T, He W, Ramakrishna S. Biomaterials 2005;26:2527-36.

[102] Ignatova M, Yovcheva T, Viraneva A, Mekishev G, Manolova N, Rashkov I. Eur Polym J 2008;44:1962-7.

[103] Kravtsov A, Brunig H, Zhandarov S, Beyreuther R. Adv Polym Tech 2000;19:312-6.

[104] Lovera D, Bilbao C, Schreier P, Kador L, Schmidt H-W, Altstaedt V. Polym Eng Sci 2009;49:2430-9.

[105] Terada A, Yuasa A, Kushimoto T, Tsuneda S, Katakai A, Tamada M. Microbiology 2006;152:3575-83.

[106] Ma Z, Kotaki M, Ramakrishna S. J Membr Sci 2005;265:115-23.

[107] Tandon V, Kirby Brian J. Electrophoresis 2008;29:1102-14.

[108] Chang I-S, Kim C-I, Nam B-U. Process Biochem 2005;40:3050-4.

[109] Bruni F, Leopold AC. Biophys J 1992;63:663-72.

[110] Yao L, Haas TW, Guiseppi-Elie A, Bowlin GL, Simpson DG, Wnek GE. Chem Mater 2003;15:1860-4.

[111] Nugen SR, Asiello PJ, Connelly JT, Baeumner Antje J. Biosens bioelectron 2009;24:2428-33.

[112] Nugen SR, Asiello PJ, Baeumner AJ. MicrosystTechnol 2009;15(3):477-83.

[113] Tsao CW, Hromada L, Liu J, Kumar P, DeVoe DL. Lab chip 2007;7:499-505.

[114] Rocha de Oliveira AA, Gomide VS, Leite MdF, Mansur HS, Pereira MdM. Mater Res (Sao Carlos, Brazil) 2009;12:239-44.

[115] Cho D, Woo JB, Joo YL, Ober CK, Frey MW. J Phys Chem C 2011; dx.doi.org /10.1021 /jp111964f.

[116] Jang J, Lee DK. Polymer 2003;44:8139-46.

[117] Mansur HS, Orefice RL, Mansur AAP. Polymer 2004;45:7193-202.

[118] Matlock-Colangelo L. in preparation 2011.

[119] Cho D, Lee S, Frey MW. Langmuir 2011;In submission.

[120] Choi S. et al. Microfluid Nanofluid (2011) 10:231–247

[121] Li L, Bellan LM, Craighead HG, Frey MW. Polymer (2006) 47(17): 6208-6217

[122] Zhou H, Kim KW, Giannelis EP, Joo YL. *Polymeric Nanofibers* (2006): 217-230

[123] Neubert S, Pliszka D, Thavasi V, Wintermantel E, Ramakrishna S. Materials Science and Engineering (2011) 176(8): 640-646

[124] Shao S, Xhou S, Li L, Li J, Luo C, Wang J, Li X, Weng J. Biomaterials (2011) 32(11): 2821-2833

[125] Mang X, Drew C, Lee S, Senecal K, Kumar J, Samuelson L. Nano Letters (2002) 2(11):1273-1275

[126] Lee Y, Lee H, Son K, Koh W. Journal of Materials Chemistry (2011) 21: 4476-4483

[127] Edwards KA, Baeumner AJ. "Liposome-enhanced Lateral-flow Assays for the Sandwich-Hybridization Detection of RNA" Book chapter in "Biosensors" Humana Press Books and Journals (accepted, 2008)

[128] Seah T, Pumera M. Sensors & Actuators B: Chemical (2011) 156(1):79-83

[129] Vamvakaki V, Fouskaki M, Chaniotakis N. Analytical Letters (2007) 40(12):2271-2287

[130] Zuwei Ma, Masaya Kotaki, Ryuji Inai and Seeram Ramakrishna.Tissue Engineering (2005)11(1-2):101-109

[131] Teh TK, Toh ST, Goh JCH. Tissue Engineering (2011) 17(6):687-703

[132] Edwards KA, Duan F, Baeumner AJ, March JC. Analytical Biochemistry (2008). 380(1):59-67